Emulsion copolymerization of styrene and butyl acrylate in the presence of a chain transfer agent. Part 1: Modeling and experimentation of batch and fedbatch processes

B. Benyahia[a,b], M. A. Latifi[a], C. Fonteix[a], F. Pla[a,*], S. Nacef[c]

[a] *Laboratoire des Sciences du Génie Chimique*
CNRS-ENSIC,1 rue Grandville, BP 20451, 54001 Nancy Cedex, France
[b] *Département de Chimie, Université Mohamed Boudiaf, M'sila, Algérie*
[c] *Département de Génie des Procédés, Université Ferhat Abbas, Sétif, Algérie*

Abstract

This paper deals with the development of a mathematical model for emulsion copolymerization of styrene and butyl acrylate carried out in the presence of n-dodecyl mercaptan as chain transfer agent (CTA). The model consisted of a system of differential algebraic equations in which the population balances is based on a new approach that reduces significantly the number of equations involved and the corresponding computational time. Most of the unknown kinetic and thermodynamic parameters of the model were estimated from experimental measurements using a stochastic optimization method based on a genetic algorithm. The results showed a fairly good agreement between model predictions and experiments. The model was then successfully validated through additional experiments carried out in batch and fedbatch reactors and clearly showed that the model was able to predict the time-evolution of overall conversion, amounts of each residual monomer, number and weight average molecular weights of the resulting copolymers and average diameters of the corresponding latex particles for different operating conditions, mainly CTA concentration and reaction temperature. The model was finally used to investigate and confirm the effects of CTA concentration, previously observed by several authors, on the kinetics of this polymerization process and on the main properties of the resulting macromolecules and latex particles.

Keywords: Emulsion copolymerization, Chain-transfer agent, Parameter identification, Modeling, Model validation, Genetic algorithm.

1. Introduction

Emulsion polymerization is an important industrial process used to produce a great variety of polymers for multiple uses (e.g. paints, adhesives, coatings, varnishes...). Moreover, it has

*Corresponding author
Email address: fernand.pla@ensic.inpl-nancy.fr (F. Pla)

[1] *Preprint submitted to Chemical Engineering Science*
[2] *Please cite this article as:*
Benyahia, B., Latifi, M. A., Fonteix, C., Pla, F., & Nacef, S. (2010). Chemical Engineering Science, 65, 850-869.

significant advantages over bulk and solution polymerization processes. These advantages result mostly from its multiphase and compartmentalized nature which allows producing, with high polymerization rates, macromolecules of high molecular weights, delivering a high versatility to product qualities. However, the complexity of emulsion polymerization systems arising from factors such as their multiphase nature, nonlinear behaviour and sensitivity to disturbances, induces more intense difficulties on modeling and makes the development of optimization procedures of emulsion polymerization reactions a very challenging task.

Molecular weight distribution (MWD), microstructure, glass transition temperature (T_g) together with particles size distribution (PSD) and morphology are the main characteristics which strongly govern the end-use properties of the resulting products (macromolecules and latex). For example, the particle size distribution (PSD) is strongly correlated to the rheological, adhesive and film-forming properties of the final products. On the other hand, MWD affects important end-use properties of the film, such as elasticity, strength, toughness, and resistance to solvents.

In radical polymerizations, molecular weights are commonly controlled using chain-transfer agents (CTAs). An ideal CTA should affect only molecular weights. However, in emulsion polymerization both molecular weights and rate of polymerization appeared to be affected by chain transfer agents. The mechanisms of radical desorption and absorption by the particles and, consequently, the particles nucleation and kinetics may be significantly modified (Barudio et al. (1998); Nomura et al. (1982); Nomura et al. (1994); Salazar et al. (1998)). It has been reported that the key feature of the CTA effect is the diffusional limitation between the different interfaces mainly droplets and water phase. As a result, the main properties of CTAs are their water solubility, their reactivity ratio and their mass transfer resistance to diffusion between phases. Mercaptans are by far the most important class of CTAs in emulsion polymerization. Several authors (Frank et al. (1948); Kolthoff and Harris (1947); Smith (1946a); Smith (1946b)) reported that mercaptans with less than 10 carbon atoms are more efficient as a result of their rapid diffusion. As a consequence they react very quickly leading to overmodifications of the macromolecules formed at the early stages and to undermodifications at the later stages because of their rapid depletion. Mercaptans with more than 10 carbon atoms are more subject to diffusional limitations and are therefore less efficient.

Mendoza et al. (2000) studied the emulsion copolymerization of styrene in the presence of n-dodecyl mercaptan. They reported that the effect of the CTA on the rate of the polymerization was weak and could be neglected.

Many contributions on the modeling of emulsion polymerization processes have been developed, starting with the conventional Smith-Ewart model (Harkins (1947)) who identified the well known three stages (nucleation, particles growth and end of polymerization). The later models developed have different degrees of complexity (Alhamad et al. (2005); Dube and Penlidis (1996); Ginsburger et al. (2003), Hoppe et al. (2005)), depending upon their scope and application. The most representative have been reviewed by Asua (2004); Chern (2006); Dube et al. (1997); Gao and Penlidis (2002) and Thickett and Gilbert (2007).

The present paper deals with the elaboration of a mathematical model for the emulsion copolymerization of styrene and butyl acrylate in the presence of n-dodecyl mercaptan as CTA. The diffusional limitations for the transfer of the CTA will be considered and its actual concentration in the particles will be evaluated. The desorption rate expression is based on a constant value of the desorption coefficient and the material balance of the oligoradicals. This approach is quite different from the expressions used in the literature where the main features of the desorption rate are gathered in the desorption coefficient expression depending on the species used in the process.

The objective of this model is to predict overall conversion, number and weight-average molecular weights, average diameter of polymer particles and residual monomers contents for different initial concentrations of CTA and reaction temperatures.
On the other hand, a novel method will be developed to carry out population balance using only two differential equations instead of the usual large number of equations used with the same accuracy. This approach will reduce significantly the computational time.

The parameters of the model will be estimated by a non linear optimization approach based on the minimization of the errors between the predictions and the measured data. This minimization will be carried out using a stochastic optimization method based on a genetic algorithm (GA).
The paper is organized as follows: in a first section the features of the model will be described highlighting the effect of the chain transfer agent and the novelties in the population balance. This will be followed by the model parameters estimation. The subsequent section will be concerned by the validation of the model and its use in order to study the effect of CTA concentration on the polymerization rate and on the properties of both the resulting copolymers and latex particles.

2. Mathematical model

Emulsion copolymerization is a free radical polymerization where the monomers are mainly located in droplets dispersed in an aqueous phase and stabilized by an excess of surfactant (mainly in its micellar form). An initiator, usually soluble in the water phase, generates primary radicals by thermal decomposition. In conventional emulsion polymerizations, monomers with low water solubility are used and lead to homogeneous and/or micellar nucleation. In the case of homogenous nucleation, the radicals propagate beyond their water solubility, precipitate and are then stabilized by the emulsifier. In the case of micellar nucleation, primary radicals enter into the micelles which are nucleated giving rise to polymer particles in which propagation, termination, inhibition and chain transfer reactions take place. The monomers needed for the reactions are provided by the droplets which act as reservoirs.

The development of the model is based on several assumptions. In this work, some of these assumptions will be made without providing justification as they are readily accepted and validated in the open literature. The remaining assumptions will be given with the necessary explanations.

The major useful assumptions can be summarized as following:

1. Only micellar nucleation is considered: the water solubility of styrene, butyl acrylate and n-C12 mercaptan is very poor (0.15, 0.3, 0.006 Kg/m^3 respectively at 25 °C). This allows considering that the polymerisation reactions take place mainly in the organic phase (the particles) and, consequently, that the homogeneous nucleation is negligible. Moreover, the surfactant concentrations used in this work are very high (>> CMC). As a result, the very important number of micelles present in the medium favours the micellar nucleation.
2. Only inhibition and initiation in the water phase are considered since the water solubility of the inhibitor is high (830 Kg/m^3 at 20 °C) and that of the initiator is practically complete under the operating conditions used.
3. Radical desorption is considered.
4. The chain transfer agent is subject to diffusional limitations mainly in the droplet-aqueous phase interface.
5. The growing particles and the monomer droplets are considered to be monodisperse.

6. Coagulation between particles is neglected.
7. Transfer to polymer reactions are not taken into account.
8. The reactor is perfectly mixed and isothermal.

It is noteworthy that the model developed in this work highlights the effect of CTA on the molecular weights and on the rate of polymerization and has the same structure as previous models elaborated in our laboratory without CTA (Hoppe et al. (2005)).

2.1. Kinetic scheme

According to aforementioned assumptions, the model is based on the elementary reactions reported in table 1.

Table 1: Kinetic scheme for the emulsion copolymerization process ($i, j = 1, 2$).

Aqueous phase	
Initiation	$I_2 \xrightarrow{k_d} 2R^{\bullet}_{aq}$
Inihibition[1]	$R^{\bullet}_{aq} + Z_{aq} \xrightarrow{k_{zaq}} P + Z^{\bullet}_{aq}$
Nucleation	$R^{\bullet}_{aq} + micelle \xrightarrow{k_N} particle + R^{\bullet}$
Radical absorption	$R^{\bullet}_{aq} + particle \xrightarrow{k_{cp}} particle + R^{\bullet}$
Organic phase	
Propagation	$R^{\bullet}_i + M_j \xrightarrow{k_{pij}} R^{\bullet}_j$
Termination by combination	$R^{\bullet}_i + R^{\bullet}_j \xrightarrow{k_{tcij}} P$
Termination by disproportionation	$R^{\bullet}_i + R^{\bullet}_j \xrightarrow{k_{tdij}} 2P$
Inihibition[1]	$R^{\bullet}_i + Z_p \xrightarrow{k_{zpi}} P + Z^{\bullet}_p$
Transfer to monomers	$R^{\bullet}_i + M_j \xrightarrow{k_{trmij}} P + R^{\bullet}_j$
Transfer to CTA	$R^{\bullet}_i + CTA_p \xrightarrow{k_{TApi}} P + CTA^{\bullet}_p$
Radical desorption	$R^{\bullet} \xrightarrow{k_{des}} R^{\bullet}_{aq}$

2.2. Reaction rates

For practical reasons, the quantities of the different species involved in the reactions will be expressed in moles number instead of concentrations. Moreover, the nomenclature of the different variables will be detailed in the nomenclature section.

2.2.1. Initiator decomposition

The initiator is consumed by thermal decomposition in the aqueous phase according to the following reaction rate:

$$\mathcal{R}_d = k_d I \tag{1}$$

[1]As mentioned in the experimental part, the monomers were used without purification. Hence, they contained traces of inhibitor (4-terbutyl catecol) which consumes radicals in both aqueous and organic phases.

2.2.2. Inhibition

The inhibitor, Z, is consumed through reactions with radicals in the aqueous phase and in the particles. The corresponding rates of consumption are:

In the aqueous phase

$$\mathcal{R}_{Zaq} = \epsilon k_{cp} \frac{Z_{aq}}{V_{aq}} R_{aq} \tag{2}$$

In the latex particles

$$\begin{aligned} \mathcal{R}_{Zpi} &= k_{Zpi} \frac{Z_p}{V_p} N_p \bar{n} P_i \\ &= k_{Zpi} \frac{Z_p}{V_p} R_{pi} \end{aligned} \tag{3}$$

where P_i is the fraction of free radicals ended by a monomer unit i such as,

$$\sum_{i=1,2} P_i = 1 \tag{4}$$

2.2.3. Chain transfer agent consumption

Only reactions with the CTA in the particles are considered:

$$\mathcal{R}_{TApi} = k_{TApi} \frac{CTA_p}{V_p} N_p \bar{n} P_i = k_{TApi} \frac{CTA_p}{V_p} R_{pi} \tag{5}$$

2.2.4. Micellar nucleation

The micellar nucleation rate is given by:

$$\mathcal{R}_N = k_N \frac{N_{mic}}{V_{aq}} R_{aq} d_{mic} \tag{6}$$

where N_{mic} is the total number of moles of micelles, d_{mic} is the micellar diameter, k_N is the nucleation rate coefficient **:**

$$k_N = \delta k_{cp} \tag{7}$$

with,

$$\delta = \sum_{i=1,2} \delta_i f_{0i} \tag{8}$$

where δ_i is the ratio between the nucleation rate constant and the capture rate constant for radicals ending with monomer i, δ is the overall ratio between nucleation and capture rate coefficients, f_{0i} is the initial molar fraction of monomer i in the reactor, k_{cp} is the capture rate coefficient.

2.2.5. Radical absorption

According to the two-film theory developed by Lewis and Whitman (1924), the absorption rate of the radicals by the particles is given by:

$$\mathcal{R}_{absi} = K_{wi}\, A_p \left(C_{wi} - C_{pi}/m_{di}\right) \tag{9}$$

$$= K_{wi}\, \pi d_p^2\, N_P\, N_A \left(\frac{R_{aq} f_{aqi}}{V_{aq}} - \frac{N_p \bar{n}}{V_p}\frac{P_i \omega_i}{m_{di}}\right) \tag{10}$$

where K_{wi} is the overall mass transfer coefficient, A_p the total surface area of the particles, C_{wi} the concentration of radicals i in the water phase, C_{pi} the concentration of radicals i in the particles.

The overall mass transfer coefficient is expressed as follows (Nomura and Harada (1981); Nomura (1982)):

$$K_{wi} = \frac{2\, D_{wi}\, \delta_{mi}}{d_p} \tag{11}$$

Hence, the absorption rate could be written as :

$$\mathcal{R}_{absi} = 2\pi D_{wi} \delta_{mi} N_A N_p d_p \left(\frac{R_{aq} f_{aqi}}{V_{aq}} - \frac{N_p \bar{n}}{V_p}\frac{P_i \omega_i}{m_{di}}\right) \tag{12}$$

$$= k_{cpi} \left(\frac{R_{aq} f_{aqi}}{V_{aq}} - \frac{N_p \bar{n}}{V_p}\frac{P_i \omega_i}{m_{di}}\right) N_p d_p \tag{13}$$

where k_{cpi} is the capture kinetic constant.

$$k_{cpi} = 2\pi N_A D_{wi} \delta_{mi} \tag{14}$$

The absorption rate is the difference between the capture and desorption rates which are respectively:

$$\mathcal{R}_{cpi} = k_{cpi} \frac{R_{aq} f_{aqi}}{V_{aq}} N_p d_p \tag{15}$$

$$\mathcal{R}_{desi} = k_{cpi} \frac{N_p \bar{n}}{V_p}\frac{P_i \omega_i}{m_{di}} N_p d_p = k_{desi} \frac{N_p \bar{n}}{V_p} \chi_i N_p d_p \tag{16}$$

where, k_{desi} is the desorption rate coefficient of the radical ended by a monomer i and χ_i the global fraction of radicals i formed by one unit of the monomer i in the particles, given respectively as follows:

$$k_{desi} = \frac{k_{cpi}}{m_{di}} \tag{17}$$

$$\chi_i = P_i \omega_i \tag{18}$$

It is noteworthy that the determination of χ_i is the key issue of the desorption rate. This has been achieved by a material balance on radicals i formed by one unit of monomer i in the particles. The differential equations obtained (see Section 2.10) show the effect of the different reactions among which the transfer to CTA.

2.2.6. Propagation

The propagation rate of monomer j with a radical ended by i is:

$$\mathcal{R}_{pij} = k_{pij}\frac{M_{pj}}{V_p}R_{pi} \tag{19}$$

which leads to the total propagation rate for monomer j:

$$\mathcal{R}_{pj} = \mathcal{R}_{pij} + \mathcal{R}_{pjj} \tag{20}$$

$$= k_{pj}\frac{M_{pj}}{V_p}N_p\bar{n} \tag{21}$$

such as,

$$k_{pj} = \sum_{i=1,2} k_{pij}P_i \tag{22}$$

and to the global propagation rate for the two monomers:

$$\mathcal{R}_p = \mathcal{R}_{p1} + \mathcal{R}_{p2} = N_p\bar{n}\sum_{j=1,2}\sum_{i=1,2} k_{pij}\frac{M_{pj}}{V_p}P_i \tag{23}$$

2.2.7. Transfer to Monomer

In the same way as for the propagation, the transfer to monomer rate of monomer j with a growing radical ended by i is given by:

$$\mathcal{R}_{trmij} = k_{trmij}\frac{M_{pj}}{V_p}R_{pi} \tag{24}$$

The total consumption rate of the monomer j by transfer reaction is then:

$$\mathcal{R}_{trmj} = \mathcal{R}_{trmij} + \mathcal{R}_{trmjj} = k_{trmj}\frac{M_{pj}}{V_p}N_p\bar{n} \tag{25}$$

where

$$k_{trmj} = \sum_{i=1,2} k_{trmij}P_i \tag{26}$$

The global transfer rate is finally given by:

$$\mathcal{R}_{trm} = \mathcal{R}_{trm1} + \mathcal{R}_{trm2} = N_p\bar{n}\sum_{j=1,2}\sum_{i=1,2} k_{trmij}\frac{M_{pj}}{V_p}P_i \tag{27}$$

The coefficients of transfer to monomer k_{trmij} and k_{trmji} are defined according to the corresponding homopolymerization transfer coefficients:

$$k_{trmij} = k_{trmji} = \sqrt{k_{trmii}k_{trmjj}} \tag{28}$$

2.2.8. Termination

The termination rate between a radical ended by a monomer i and a radical ended by a monomer j is:

$$\mathcal{R}_{Tij} = k_{Tij} P_i P_j \frac{N_p^2}{V_p} \tilde{n} \tag{29}$$

$$= \frac{k_{Tij} R_{pi} R_{pj} \tilde{n}}{V_p \bar{n}^2} \tag{30}$$

$\bar{n}$, $\tilde{n}$ are the average numbers of radicals and pairs of radicals in a particle respectively given by:

$$\tilde{n} = \sum_{h=2}^{\infty} h(h-1)\upsilon_h \tag{31}$$

$$\bar{n} = \sum_{h=2}^{\infty} h\upsilon_h \tag{32}$$

where h and υ_h are the number of free radicals in a particular particle and the fraction of particles with h free radicals, with:

$$\sum_{h=2}^{\infty} \upsilon_h = 1 \tag{33}$$

The global termination rate is defined as:

$$\mathcal{R}_T = \mathcal{R}_{T11} + \mathcal{R}_{T12} + \mathcal{R}_{T21} + \mathcal{R}_{T22} = k_T \frac{N_p^2}{V_p} \tilde{n} \tag{34}$$

where k_T is the overall termination rate coefficient given by:

$$k_T = \sum_{j=1,2} \sum_{i=1,2} k_{Tij} P_i P_j \tag{35}$$

According to the assumption that the kinetic coefficients do not depend on the chain length, it is acceptable to consider that the termination coefficients between a radical ended by a monomer unit i and a radical ended by a monomer unit j are equal.

$$k_{Tij} = k_{Tji} \tag{36}$$

These coefficients are calculated using the homopolymerization termination coefficients of the monomers:

$$k_{Tij} = k_{Tji} = \sqrt{k_{Tii} k_{Tjj}} \tag{37}$$

The ratio between the rates of termination by disproportionation and by combination is defined by a coefficient τ. Since the global termination rate is the sum of the two mechanisms, the rates of termination by combination and by disproportionation are given respectively by:

$$\mathcal{R}_{TC} = \frac{\mathcal{R}_T}{1+\tau} \tag{38}$$

$$\mathcal{R}_{TD} = \frac{\tau \mathcal{R}_T}{1+\tau} \tag{39}$$

2.3. Partition of the different species

2.3.1. Surfactant

The surfactant is distributed between the particles, the droplets, the aqueous phase and the micelles. The total number of moles of surfactant in the reactor is given by:

$$S = S_{aq} + S_{mic} + S_p + S_d \tag{40}$$

where S_p , S_{mic}, S_d and S_{aq} are the number of moles of surfactant on the particles, in the micelles, on the droplets and dissolved in the aqueous phase, respectively. They are calculated using the following equations:

$$S_{mic} = N_{mic} n_s \tag{41}$$

$$S_p = \frac{6V_p}{d_p a_s} \tag{42}$$

$$S_d = \frac{6V_d}{d_d a_s} \tag{43}$$

where N_{mic} is the total number of moles of micelles, n_s the number of surfactant molecules per micelle, a_s the surface covered by one mole of surfactant, d_d the droplets average diameter. The total number of moles in the aqueous phase is given as follows,

$$\begin{aligned} S^*_{aq} &= S_{aq} + S_{mic} \\ &= S - (S_p + S_d) \end{aligned} \tag{44}$$

The micelles disappear when the concentration of surfactant in the aqueous phase becomes lower than the critical micellar concentration (CMC). Thus:

if $S^*_{aq} < CMC \cdot V_{aq}$ then

$$N_{mic} = 0 \tag{45}$$

$$S_{aq} = S^*_{aq} \tag{46}$$

otherwise

$$S_{aq} = CMC \cdot V_{aq} \tag{47}$$

$$N_{mic} = \frac{S - \left(S_d + S_p + CMC \cdot V_{aq}\right)}{n_s} \tag{48}$$

2.3.2. Monomers, inhibitor and CTA

The partition of the different species between the aqueous phase, particles and droplets is needed to evaluate the reaction rates. This has been performed using the method by Gugliotta et al. (1995) (see Appendix A).
Let us consider the total volume engaged in the reactor V_R expressed by means of the total volume of each specie and different phases:

$$\begin{aligned} V_R &= V_1 + V_2 + V_Z + V_{CTA} + V_{pol} + V_w \\ &= V_{aq} + V_p + V_d \end{aligned} \tag{49}$$

where V_1, V_2, V_Z, V_{CTA}, V_{pol} and V_w are the total volumes of monomer 1, monomer 2, inhibitor, CTA, polymer and water volumes respectively.
Moreover, the particles and the polymer volumes are related to each other by:

$$V_p = \left(\frac{\sigma}{\sigma - 1}\right) V_{pol} \tag{50}$$

where σ is a coefficient of partition of the different species between droplets and particles and V_{pol} is given by:

$$V_{pol} = \sum_{i=1,2} \left(M_{Ti} - M_i - R_{aq} f_{aqi}\right) \frac{M_M^i}{\rho_{pi}} \tag{51}$$

Since the solubility of each specie in the aqueous phase is very low, the volume of the aqueous phase is equivalent to the water volume (V_w),

$$V_{aq} \cong V_w \tag{52}$$

Hence, from equations (49) and (50) the droplets volume is:

$$V_d = V_1 + V_2 + V_Z + V_{CTA} - \frac{V_{pol}}{1 - \sigma} \tag{53}$$

When the droplets disappear, equations (49) and (50) lead to the expression of the particles volume V_p:

$$V_p = V_1 + V_2 + V_Z + V_{CTA} + V_{pol} \tag{54}$$

Finally, the partition problem can be summarized as follows:
if the droplets are available:

$$\begin{aligned} V_d &= V_1 + V_2 + V_Z + V_{CTA} - \frac{V_{pol}}{1 - \sigma} \\ V_p &= \left(\frac{\sigma}{\sigma - 1}\right) V_{pol} \end{aligned} \tag{55}$$

otherwise:

$$\begin{aligned} V_d &= 0 \\ V_p &= V_1 + V_2 + V_Z + V_{CTA} + V_{pol} \end{aligned} \tag{56}$$

It should be emphasized that in all cases the aqueous volume is determined from the volume balance:

$$V_{aq} = V_R - V_d - V_p \tag{57}$$

The total number of moles of the monomers and the inhibitor necessary to the feed rates considered under thermodynamic equilibrium are: (see Appendix A)

$$M_{pi} = \frac{M_i V_p}{\left(V_p + V_d\sigma + V_{aq}K_{pi}\right)} \tag{58}$$

$$Z_p = \frac{ZV_p}{\left(V_p + V_d\sigma + V_{aq}K_{pZ}\right)} \tag{59}$$

$$Z_{aq} = K_{pz}Z_p\frac{V_{aq}}{V_p} \tag{60}$$

$$f_{aqi} = \frac{K_{pi}M_p^i}{\sum\limits_{j=1,2} K_{pj}M_p^j} \tag{61}$$

Where M_{pi}, Z_p are the total number of moles of monomer i and inhibitor respectively in the particles, Z_{aq} the concentrations of the inhibitor in the aqueous phase, f_{aqi} the molar fraction of monomer i in the aqueous phase.
For the chain transfer agent, the diffusion from the droplets to the aqueous phase is the limiting step. The expression derived for the number of moles of CTA in the particle is similar to that obtained by Salazar et al. (1998) for emulsion polymerization. (see Appendix B)

$$CTA_p = \frac{CTA_p^e}{1 + \dfrac{k_{TA1}R_{p1} + k_{TA2}R_{p2}}{k_{TA,dw}A_dK_{pTA}}} \tag{62}$$

where CTA_p^e is the number of CTA moles in the particles supposed in thermodynamic equilibrium,

$$CTA_p^e = \frac{CTA\ V_p}{\left(V_p + V_d\sigma + V_{aq}K_{pTA}\right)} \tag{63}$$

2.4. Influence of temperature

The effect of temperature on the kinetic constants is expressed by Arrhenius' law. On the other hand and according to Gilbert's assumptions (Gilbert (1995)), the specific area of a surfactant molecule depends on the temperature and could be expressed by an exponential formula similar to Arrhenius' law:

$$a_e(T) = a_e(323.15)exp\left(-E_e\left(\frac{1}{T} - \frac{1}{323.15}\right)\right) \tag{64}$$

where E_e is the thermal expansion factor of a surfactant molecule.

2.5. Initiator efficiency

The initiator efficiency, f, can strongly depend on the type and on the monomer concentration (Gilbert (1995)). Usually, efficiencies of 30 and 100 are attributed to persulphates when they are used with styrene and butyl acrylate respectively. In order to describe the transition between these values, the following formula was used:

$$f = exp\left(-f_0 f_b\right) \tag{65}$$

where f_0 is a parameter to be fitted and f_b is the fraction of styrene in the reactor.

2.6. Glass and gel effects

Glass and gel effects equations used to determine the propagation and termination coefficients are expressed according to the value of the mass fraction of polymer in the particles, W_p (Nomura et al. (1994)) (see table (2).

Table 2: Glass and gel effects.

if $W_p \leq 0.7$	$k_{pij} = k^0_{pij}$
if $W_p > 0.7$	$k_{pij} = k^0_{pij} \exp\left(-a^{Gl}_{ij}\left(W_p - 0.7\right)\right)$
if $W_p \leq 0.32$	$k_{Tij} = k^0_{Tij}$
if $0.32 < W_p \leq 0.8$	$k_{Tij} = k^0_{Tij} \exp\left(-b^{Ge}\left(W_p - 0.32\right)\right)$
if $W_p > 0.8$	$k_{Tij} = k^0_{Tij} \exp\left(-b^{Ge}\left(0.8 - 0.32\right) - b^{Gl}\left(W_p - 0.8\right)\right)$

W_p is defined as:

$$W_p = \frac{\sum\limits_{i=1,2}\left(M_{Ti} - M_i - R_{aq} f_{aqi}\right) M^i_M}{\sum\limits_{i=1,2}\left(M_{pi} + M_{Ti} - M_i - R_{aq} f_{aqi}\right) M^i_M} \tag{66}$$

2.7. Conversion and copolymer composition

The overall mass conversion and the residual mass fraction of monomer i are given by:

$$X_{ove} = \frac{\sum_{i=1,2} (M_{Ti} - M_i) M_M^i}{\sum_{i=1,2} M_{Ti} M_M^i} \tag{67}$$

$$F_i = \frac{M_i M_M^i}{\sum_{j=1,2} M_j M_M^j} \tag{68}$$

2.8. Population balance for polymer particles

In order to evaluate the reaction rates, one must know the average number of radicals per particle. This was obtained by performing balances on the number of particles containing, at any instant, j radicals. On the other hand, since each transfer agent reaction consumes and simultaneously provides one free radical, it has no effect on the distribution of the radicals in the particle. The balance equations of particles containing j radicals are:

particles containing 0 *radical*

$$\frac{d(N_P \upsilon_0)}{dt} = -\mathcal{R}_{cp}\upsilon_0 + \frac{\mathcal{R}_T}{\tilde{n}}\upsilon_2 + \left(\mathcal{R}_{Zp} + \mathcal{R}_{des}\right)\frac{\upsilon_1}{\bar{n}} \tag{69}$$

particles containing 1 *radical*

$$\begin{aligned} \frac{d(N_P \upsilon_1)}{dt} &= \mathcal{R}_N + 3\frac{\mathcal{R}_T}{\tilde{n}}\upsilon_3 - \mathcal{R}_{cp}\upsilon_1 + \mathcal{R}_{cp}\upsilon_0 \\ &+ \left(\mathcal{R}_{Zp} + \mathcal{R}_{des}\right)\frac{(2\upsilon_2 - \upsilon_1)}{\bar{n}} \end{aligned} \tag{70}$$

particles containing h radical (h > 1)

$$\begin{aligned} \frac{d(N_P \upsilon_h)}{dt} &= \mathcal{R}_{cp}(\upsilon_{h-1} - \upsilon_h) \\ &+ \frac{\mathcal{R}_T}{2\tilde{n}}\left((h+2)(h+1)\upsilon_{h+2} - h(h-1)\upsilon_h\right) \\ &+ \left(\mathcal{R}_{Zp} + \mathcal{R}_{des}\right)\frac{((h+1)\upsilon_{h+1} - h\upsilon_h)}{\bar{n}} \end{aligned} \tag{71}$$

where υ_h is the fraction of particles containing h radicals.

To determine the average number of radicals per particle ($\bar{n}$) and the average number of pairs ($\tilde{n}$) necessary for the calculation of the termination rates, a maximum number of radicals per particle (j_{max}) has to be fixed (Ginsburger et al. (2003); Storti et al. (1989)). This approach implies to deal with j_{max} differential equations where the accuracy of the results depends on the choice of j_{max} . To avoid this procedure, we suppose that the fraction of particles containing j

free radicals follows Poisson's law (see Appendix C). Thanks to this approach, we obtain the two following differential equations:

$$\frac{d\left(N_p\bar{n}\right)}{dt} = \mathcal{R}_N + \mathcal{R}_{cp} - \left(\mathcal{R}_{Zp} + \mathcal{R}_T + \mathcal{R}_{des}\right) \tag{72}$$

$$\frac{d\left(N_P\tilde{n}\right)}{dt} = 2\mathcal{R}_{cp}\bar{n} - \left(\frac{2\tilde{\bar{n}}}{\tilde{n}} + 1\right)\mathcal{R}_T - 2\frac{\tilde{n}}{\bar{n}}\left(\mathcal{R}_{Zp} + \mathcal{R}_{des}\right) \tag{73}$$

$$\tilde{\bar{n}} = \tilde{n}\left[\frac{\lambda\left(1 + \frac{\tilde{n}}{\bar{n}}\right) + \frac{\tilde{n}}{\bar{n}}}{\lambda + 2}\right] \tag{74}$$

$$\lambda = \frac{\tilde{n}}{2\bar{n}} - 1 + \sqrt{1 + \frac{\tilde{n}}{4\bar{n}}} \tag{75}$$

2.9. Average molecular weights

The physical and mechanical properties of polymers depend strongly on their molecular weight distributions (MWD). Therefore, one of the aims of the model is to determine this characteristic. This was achieved by using the method of the moments (Baillagou and Soong (1985); Villermaux and Blavier (1984)). To apply this method, a description of the evolution of the instantaneous distributions of the degree of polymerization of both macroradicals and macromolecules is required. The k^{th} normalized moments of the macroradicals and the macromolecules are given respectively by:

$$\lambda_k = \sum_{j=1}^{\infty} j^k \bar{w}_j \tag{76}$$

$$L_k = \sum_{j=1}^{\infty} j^k w_j \tag{77}$$

where $\bar{w}_j$ and w_j are the fraction of macroradicals and macromolecules with a degree of polymerization j respectively.
The corresponding balance equations are:

$$\begin{aligned}\frac{d\left(N_p\bar{n}\lambda_1\right)}{dt} &= \mathcal{R}_N + \mathcal{R}_{cp} - \mathcal{R}_{des} + \mathcal{R}_p + \left(\mathcal{R}_{trm} + \mathcal{R}_{TAp}\right) \\ &\quad (1 - \lambda_1) - \left(\mathcal{R}_{Zp} + \mathcal{R}_T\right)\lambda_1\end{aligned} \tag{78}$$

$$\begin{aligned}\frac{d\left(N_p\bar{n}\lambda_2\right)}{dt} &= \mathcal{R}_N + \mathcal{R}_{cp} - \mathcal{R}_{des} + \mathcal{R}_p\left(1 + 2\lambda_1\right) \\ &+ \left(\mathcal{R}_{trm} + \mathcal{R}_{TAp}\right)(1 - \lambda_2) - \left(\mathcal{R}_{Zp} + \mathcal{R}_T\right)\lambda_2\end{aligned} \tag{79}$$

$$\frac{d\left(N_m\right)}{dt} = \mathcal{R}_{Zp} + \mathcal{R}_{trm} + \mathcal{R}_{TD} + \mathcal{R}_{TAp} + \frac{\mathcal{R}_{TC}}{2} \tag{80}$$

$$\frac{d\left(N_m L_1\right)}{dt} = \lambda_1 \left(\mathcal{R}_{Zp} + \mathcal{R}_{trm} + \mathcal{R}_{TD} + \mathcal{R}_{TAp} + \mathcal{R}_{TC}\right) \tag{81}$$

$$\begin{aligned} \frac{d\left(N_m L_2\right)}{dt} &= \lambda_2 \left(\mathcal{R}_{Zp} + \mathcal{R}_{trm} + \mathcal{R}_{TD} + \mathcal{R}_{TAp}\right) \\ &+ \mathcal{R}_{TC} \left(\lambda_2 + \lambda_1^2\right) \end{aligned} \tag{82}$$

The initial conditions for the equations of moments are given by,
$\lambda_1 = 0, \lambda_2 = 0, N_m = 0, L_1 = 0, L_2 = 0$
The number and weight average molecular weights, $\bar{M}_n$ and $\bar{M}_w$ can be easily calculated by using the following equations:

$$\bar{M}_n = \bar{M} L_1 \tag{83}$$

$$\bar{M}_w = \bar{M} \frac{L_2}{L_1} \tag{84}$$

where $\bar{M}$ is the average molecular weight of the monomeric unit given by

$$\bar{M} = \frac{\sum\limits_{i=1,2} \left(M_{Ti} - M_i - R_{aq} f_{aqi}\right) M_M^i}{\sum\limits_{i=1,2} \left(M_{Ti} - M_i - R_{aq} f_{aqi}\right)} \tag{85}$$

2.10. Material balance

The material balances are presented in a general form for fedbatch process using the reaction rates mentioned above. These equations could be easily simplified for the case of a batch process.

$$\frac{dV_R}{dt} = Q_f + Q_{If} + \sum_{i=1,2} \left(\frac{1}{\rho_{pi}} - \frac{1}{\rho_i}\right) M_M^i \left(\mathcal{R}_{pi} + \mathcal{R}_{trmi}\right) \tag{86}$$

$$\frac{dM_i}{dt} = -\mathcal{R}_{pi} - \mathcal{R}_{trmi} + Q_f \left[M_i\right]_f \tag{87}$$

$$\frac{dM_{Ti}}{dt} = Q_f \left[M_i\right]_f \tag{88}$$

$$\frac{dI}{dt} = -\mathcal{R}_d + Q_{If} \left[I\right]_f \tag{89}$$

$$\frac{dZ}{dt} = -\left(\mathcal{R}_{Zp1} + \mathcal{R}_{Zp2}\right) + Q_f \left[Z\right]_f \tag{90}$$

$$\frac{dCTA}{dt} = -\mathcal{R}_{TAp1} - \mathcal{R}_{TAp2} + Q_f \left[CTA\right]_f \tag{91}$$

$$\frac{dS}{dt} = Q_f \left[S\right]_f \tag{92}$$

$$\frac{dN_p}{dt} = \mathcal{R}_N \tag{93}$$

$$\frac{d\left(N_p\bar{n}\right)}{dt} = \mathcal{R}_N + \mathcal{R}_{cp} - \left(\mathcal{R}_{Zp} + \mathcal{R}_T + \mathcal{R}_{des}\right) \tag{94}$$

$$\begin{aligned}\frac{d\left(N_P\tilde{n}\right)}{dt} &= 2\mathcal{R}_{cp}\bar{n} - \left(\frac{2\tilde{\bar{n}}}{\tilde{n}} + 1\right)\mathcal{R}_T \\ &- 2\frac{\tilde{n}}{\bar{n}}\left(\mathcal{R}_{des} + \mathcal{R}_{TAp}\right)\end{aligned} \tag{95}$$

$$\begin{aligned}\frac{dR_{p1}}{dt} &= \left(\mathcal{R}_N + \mathcal{R}_{cp}\right) f_{aq1} - \mathcal{R}_{p12} + \mathcal{R}_{p21} - \mathcal{R}_{trm12} \\ &+ \mathcal{R}_{trm21} - \mathcal{R}_{Zp1} - \mathcal{R}_{des1} - \left(\mathcal{R}_{T11} + \mathcal{R}_{T12}\right)\end{aligned} \tag{96}$$

$$\begin{aligned}\frac{dR_{p2}}{dt} &= \left(\mathcal{R}_N + \mathcal{R}_{cp}\right) f_{aq2} - \mathcal{R}_{p21} + \mathcal{R}_{p12} - \mathcal{R}_{trm21} \\ &+ \mathcal{R}_{trm12} - \mathcal{R}_{Zp2} - \mathcal{R}_{des2} - \left(\mathcal{R}_{T22} + \mathcal{R}_{T21}\right)\end{aligned} \tag{97}$$

$$\begin{aligned}\frac{d\left(N_P\bar{n}\chi_1\right)}{dt} &= \left(\mathcal{R}_N + \mathcal{R}_{cp}\right) f_{aq1} + \mathcal{R}_{trm21} + \mathcal{R}_{trm11} \\ &+ \mathcal{R}_{TAp1} - \mathcal{R}_{des1} - \left(\mathcal{R}_{trm11} + \mathcal{R}_{trm12}\right. \\ &+ \left.\mathcal{R}_{p11} + \mathcal{R}_{p12} + \mathcal{R}_{TAp1} + \mathcal{R}_{Zp1}\right)\chi_1 \\ &- \left(\mathcal{R}_{T11} + \mathcal{R}_{T12}\right)\chi_1\end{aligned} \tag{98}$$

$$\begin{aligned}\frac{d\left(N_P\bar{n}\chi_2\right)}{dt} &= \left(\mathcal{R}_N + \mathcal{R}_{cp}\right) f_{aq2} + \mathcal{R}_{trm12} + \mathcal{R}_{trm22} \\ &+ \mathcal{R}_{TAp2} - \mathcal{R}_{des2} - \left(\mathcal{R}_{trm22} + \mathcal{R}_{trm21}\right. \\ &+ \left.\mathcal{R}_{p22} + \mathcal{R}_{p21} + \mathcal{R}_{TAp2} + \mathcal{R}_{Zp2}\right)\chi_2 \\ &- \left(\mathcal{R}_{T22} + \mathcal{R}_{T21}\right)\chi_2\end{aligned} \tag{99}$$

where, Q_f is the preemulsion feed rate (monomers, inhibitor, CTA and surfactant), Q_{If} the initiator feed rate of, ρ_{pi} the density of the homopolymer i. $[M_i]_f$, $[I]_f$, $[Z]_f$, $[S]_f$, $[CTA]_f$ the concentrations of monomer i, initiator, inhibitor, surfactant and CTA in the feed.
The initial conditions for the balane equations are given by,
$V_R = \left(V_{aq0} + \frac{m_{10}}{\rho_1} + \frac{m_{20}}{\rho_2} + \frac{m_{S0}}{\rho_S}\right)$, $M_1 = \frac{m_{10}}{M_M^1}$, $M_2 = \frac{m_{20}}{M_M^2}$, $M_{T1} = \frac{m_{10}}{M_M^1}$, $M_{T2} = \frac{m_{20}}{M_M^2}$, $I = \frac{m_{I0}}{M_M^I}$, $Z = \left(\frac{m_{10}}{M_M^1} + \frac{m_{20}}{M_M^2}\right)15e^{-6}$, $CTA = \frac{m_{CTA0}}{M_M^{CTA}}$, $S = \frac{m_{S0}}{M_M^S}$, $N_p = 0$, $\bar{n} = 0$, $\tilde{n} = 0$, $R_{p1} = 0$, $R_{p2} = 0$, $\chi_1 = 0$, $\chi_2 = 0$
where V_{aq0} is the initial water volume, m_{10}, m_{20}, m_{I0}, m_{CTA0}, m_{S0} are the initial mass of monomer 1, monomer 2, initiator, CTA and surfactant respectively

3. Experimental rig and measurement

3.1. Initial components

The chemicals required to carry out the emulsion copolymerizations consisted of:
Monomers : Styrene (STY) and butyl acrylate (ABu) previously stabilized with 15 ppm of 4-terbutylcatechol(inhibitor), purchased from ACROS ORGANICS.
Initiator : Ammonium persulphate ($(NH_4)_2S_2O_8$) purchased from Sigma-Aldrich.
Surfactant : REWOPOL SBFA 50 (sulfosuccinate polyetherglycol and alcohol disodium) purchased from Goldschmidt.
Chain transfer agent : n-dodecyl mercaptan purchased from ACROS ORGANICS.
Water : the water used is purified to Milli-Q standard.
Inhibitor: Hydroquinone used to quench the polymerisation in withdrawn samples.
Solvent: Tetrahydrofuran used for size exclusion chromatography (SEC) and gas chromatography (GC).

3.2. Experimental rig

The reactor used was a one-litter jacketed glass reactor equipped with a stainless steel stirrer, a reflux condenser, a cryostat, a nitrogen inlet and a sampling device. The stirrer was composed of a pitch blade turbine fixed at the bottom. Its rotation speed was kept constant at 200 rpm. For fedbatch experiments, this reactor was connected to a second 1 liter reactor in which monomers, chain transfer agent and surfactant were pre-emulsified. The pre-emulsion was then added to the polymerization reactor by use of a peristaltic pump. Under these conditions the mixture appeared to be homogenous and the temperature was maintained constant during each experiment. Samples were withdrawn from the reactor at appropriate time intervals and polymerization was shortly stopped with hydroquinone at low temperature. Tables (3) and (4) present the formulations used for batch and fedbatch experiments respectively.

Table 3: Formulations used in batch copolymerizations.

Species	R1	R2	R3	R4	V1	V2	V3
Butyl acrylate, (g)	60	60	60	60	60	60	60
Styrene, (g)	60	60	60	60	60	60	60
Initiator, $(NH_4)_2S_2O_8$ (g)	1	1	1	1	1	1	1
Water, (g)	570	570	570	570	570	570	570
REWOPOL SBFA 50, (g)	15	15	15	15	15	15	15
n-C12 mercaptan (CTA), (g)	0.3	0.6	0.3	0.6	0.45	1.5	2.1
$m_{CTA}/m_{monomers}$, (%)	0.25	0.5	0.25	0.5	0.375	1.25	1.75
Temperature, (°C)	60	60	70	70	65	70	70

In table (3) R1 to R4 represent the experiments used for the parameter identification and V1 to V3 the experiments used for model validation in batch conditions.

3.2.1. Characterization of lattices and macromolecules

To follow the polymerizations, analytical methods were developed. The recovered samples were characterized as follows:

Table 4: Formulation used in fedbatch polymerization.

Species	Initial charge	Feed charge
Butyl acrylate, (g)	18	42
Styrene, (g)	18	42
Initiator,$(NH_4)_2S_2O_8$ (g)	1	0
REWOPOL SBFA 50, (g)	4.5	10.5
Water, (g)	171	399
n-C12 mercaptant (CTA), (g)	0.18	0.42
$m_{CTA}/m_{monomers}$, (%)	5	5
Temperature, (°C)	70	

Overall conversion:
The global monomer conversion X_{ove}, was determined gravimetrically using a Mettler Toledo HG 53 halogen moisture analyzer. About 1 g of latex was placed on an aluminum plate that was introduced into the analyser and heated to 175 °C to evaporate completely water and residual monomers. The mass of the final dried sample was automatically measured. After correction of the remaining amounts of initiator and surfactant, the overall conversion was determined.

Residual monomers titration:
For a better control of the consumption of each monomer during the polymerization, a more precise titration of the monomers is required. To get these informations, gas chromatography was performed using a VARIAN GC3900 gas chromatograph equipped with a capillary column (length :15 m ; diameter : 0.53 μm) and with a stainless steel precolumn filled up with glass fibers. Analyses were carried out under the following operating conditions:

- Injection temperature : 175 °C.
- Column temperature : 80 °C.
- Detector temperature : 175 °C.
- Gas vector : Helium (flow-rate = 3 $ml.min^{-1}$).

Average particles diameters:
The average particles diameters were determined by use of a Malvern 4700 quasi-elastic light scattering apparatus. After dilution of the samples with deionized water (milli-Q water), the average particles diameter was measured.
It should be noted that the corresponding distributions of the particles diameters were very narrow which confirms the hypothesis given in section 2.

Number and weight average molecular weights:
The number and weight average molecular weights were determined by size exclusion chromatography (SEC) using a differential refractometer as detector. Elutions were performed at 25 $^{\circ}C$ with tetrahydrofuran. The flow rate was $1ml \cdot min^{-1}$. The concentration of the polymer solutions and the corresponding injected volume were 1 $g.l^{-1}$ and 25 μl respectively. Prior to chromatography, THF and polymer solutions were filtered through a Nylon filter of 0.45 μm porosity.

The SEC device consisted of a degaser, a differential refractometer Waters 510, Millipore pump, a Millipore injector, a precolumn, two chromatographic columns assembled in series and filled with linear ultrastyragel and an electric oven to control the temperature of the columns which were previously calibrated with polystyrene standards. Data from the detector were acquired and computed by means of the software Astra from Wyatt Technology which allowed determining the molecular weight distribution and the number and weight average molecular weights of the samples.

4. Results and discussion

4.1. Parameters estimation

The goal of the model was to predict satisfactorily and simultaneously the overall conversion (X_{ove}), the residual mass fraction of styrene (F_2), the number and weight average molecular weights ($\bar{M}_n$, $\bar{M}_w$) and the average particles diameters (d_p).

It is well known that a first step, prior to the parameters identification, consists in determining the subset of potentially estimable parameters. Moreover, due to the model structure and to a possible lack of measurements, the estimation of some parameters may be impossible. The main limitations to the parameters estimability are their weak effect on the measured outputs and the correlation between these effects.
We have developed a sensitivity analysis method to identify the subset of potentially estimable parameters from the proposed experimental data. This procedure is beyond the scope of this paper and will be developed in more details in the next contribution. As a result 21 parameters were selected among the 49 parameters of the model. The 28 other parameters were taken from the litterature (table (5)). The 21 unknown parameters, listed in table (6), were determined by minimizing of the maximum likelihood criterion J defined as the logarithm of the sum of square differences between experimental measurements and model predictions (Walter and Pronzato (1994)):

$$J = \sum_{k=1}^{5} N_k ln\left(\sum_{l=1}^{N_k} (x_k(t_{kl}) - \hat{x}_k(t_{kl}, \theta))^2\right) \tag{100}$$

where N_k is the number of measurements of the variables x_k, t_{kl} is the lth time of measurement of the variable x_k (Table (7)), and $\hat{x}_k$ is the value of x_k predicted by the model using the values θ of the unknown parameters. In this relation, the five variables x_k were : X, M_n, M_w, d_p and F_2.

The 21 unknown parameters of the (vector θ) were simultaneously obtained by minimization of J using a stochastic optimization method based on a genetic algorithm and the code DASSL for the system integration.
The measurements used in the parameter identification are obtained from batch experiments R1 to R4 listed in table (3). The resulting optimized values, presented in table (6), are of the same order of magnitude as the values found in the literature (Ginsburger et al. (2003), Hoppe et al. (2005)). Moreover, the reactivity ratio between CTA and styrene ($C_{CTA,2} = k_{TAp20}/k_{p220}$) is 1.14. Salazar et al. (1998) reported values varying from 0.31 to 2.2 for this parameter in the case of different emulsion polymerizations.

Table 5: Parameters from the literature.

Parameter	Value	Units	Reference
E_d	135 000	$J \cdot mol^{-1}$	Gilbert (1995)
E_{p11}	22 500	$J \cdot mol^{-1}$	Ginsburger et al. (2003)
E_{p22}	32 500	$J \cdot mol^{-1}$	Gilbert (1995)
E_{t22}	9000	$J \cdot mol^{-1}$	Sgard (2000)
E_{trm11}	20 000	$J \cdot mol^{-1}$	Ginsburger et al. (2003)
m_{d1}, m_{d2}	39		Rawlings and Ray (1988)
n_s	40		Ginsburger et al. (2003)
E_e	361	K	Ginsburger et al. (2003)
δ_{m1}, δ_{m2}	0.03		Ginsburger et al. (2003)
δ_1	31		Ginsburger et al. (2003)
δ_2	22		Ginsburger et al. (2003)
K_{p1}	1/1050		Gugliotta et al. (1995)
K_{p2}	1/2512		Gugliotta et al. (1995)
r_{mic}	2.5	nm	Gilbert (1995)
r_d	5000	nm	Gilbert (1995)
D_{w1}, D_{w2}	$4.1 \cdot 10^{-7}$	$m^2 \cdot s^{-1}$	Arzamendi et al. (1992)
a_{11}^{gl}	17.13		Martinet (1992)
a_{12}^{gl}	5.73		Martinet (1992)
a_{21}^{gl}	5.73		Martinet (1992)
a_{22}^{gl}	5.73		Martinet (1992)
b^{ge}	11.46		Martinet (1992)
b^{gl}	3.78		Martinet (1992)
a_e	0.75	nm^2	Ginsburger et al. (2003)
$k_{TA,dw}A_d$	5/6	$m^3 \cdot s^{-1}$	Salazar et al. (1998)
τ	2/3		Ginsburger et al. (2003)

Table 6: Results of the parametric identification.

Parameter	Signification	Value
k_{zp}	Inhibition constant in particles $m^3 \cdot kmol^{-1} \cdot s^{-1}$	150
k_{TAp10}	Transfer rate coefficient, CTA to butyle acrylate at 50°C, $m^3 \cdot kmol^{-1} \cdot s^{-1}$	47
k_{TAp20}	Transfer rate coefficient, CTA to to styrene at 50°C, $m^3 \cdot kmol^{-1} \cdot s^{-1}$	409
E_{TAp1}	Activation energy of transfer , CTA to butyle acrylate $Kj/kmol$	63 000
E_{TAp2}	Activation energy of transfer , CTA to styrene $Kj/kmol$	34 000
k_{p110}	Propagation rate coefficient of butyle acrylate at 50°C, $m^3 \cdot kmol^{-1} \cdot s^{-1}$	286
k_{p220}	Propagation rate coefficient of styrene at 50°C, $m^3 \cdot kmol^{-1} \cdot s^{-1}$	359
k_{t110}	Termination rate coefficient of butyle acrylate at 50°C , $m^3 \cdot kmol^{-1} \cdot s^{-1}$	$89{\cdot}10^8$
k_{t220}	Termination rate coefficient of styrene at 50°C , $m^3 \cdot kmol^{-1} \cdot s^{-1}$	$39{\cdot}10^8$
E_{t11}	Activation energy of monomer 2 termination $Kj/kmol$	130 000
k_{trm110}	Transfer constant of butyle acrylate at 50°C, $m^3 \cdot kmol^{-1} \cdot s^{-1}$	0.05
k_{trm220}	Transfer constant of styrene at 50°C, $m^3 \cdot kmol^{-1} \cdot s^{-1}$	0.018
E_{trm22}	Activation energy of transfer to styrene $Kj/kmol$	34 700
k_{d0}	Initiator decomposition constant at 50°C, s^{-1}	$5.5{\cdot}10^{-6}$
K_{pZ}	Partition coefficient of the inhibitor between the droplets and the aqueous phase	1.7
K_{pta}	Partition coefficient of the CTA between the droplets and the aqueous phase	0.55
r_{p12}	Reactivity ratio of butyl acrylate	0.18
r_{p21}	Reactivity ratio of styrene	0.78
σ	Swelling parameters of the particles	1.03
f_0	A parameter related to the initiator efficiency	0.88
ϵ	Ratio of inhibition in aqueous phase and capture rate coefficients, m	10.21

Table 7: Number of measurements for each variable x_k.

Experiment	X_{ove}	$\bar{M}_n$	$\bar{M}_w$	d_p	F_2
$Run1$	9	8	6	9	7
$Run2$	8	9	9	9	7
$Run3$	9	8	8	9	7
$Run4$	9	7	6	10	7
$N_k(total)$	35	32	29	37	28

4.2. Associated results

As shown in table 3, the measured data were obtained from several batch emulsion copolymerizations carried out at different temperatures, with identical initial initiator, Styrene and Butyl acrylate masses and with different chain transfer agent concentrations.

Overall monomers conversion

Figure (1) shows that a good agreement was obtained between experimental and simulated time-evolution curves of the global monomers conversion. As expected, these curves clearly show that the conversion rate increases with temperature. On the other hand, with the CTA concentrations used in these experiments, it can be seen that the chain transfer agent has only a very slight effect on the polymerization rate. Similar results were found for styrene emulsion polymerization by Mendoza et al. (2000). Nevertheless, in investigations on the efficiency of different mercaptan CTAs in styrene/butyl acrylate emulsion copolymerization, Barudio et al. (1998) observed a decrease of the polymerization rate as the CTAs concentration was increased. Moreover, the authors found that this effect became more pronounced as the number of carbon atoms of the mercaptan decreased.

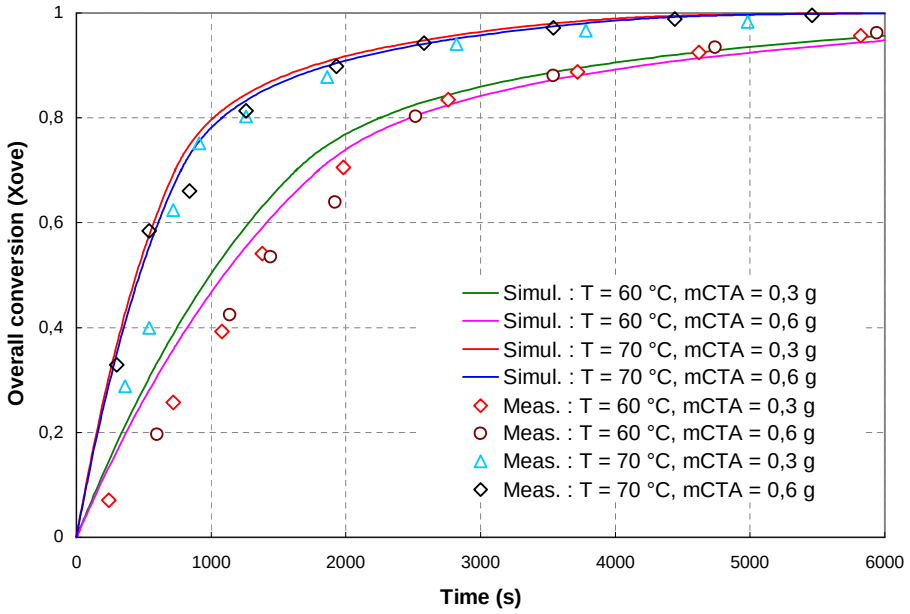

Figure 1: Effect of CTA concentration and reaction temperature on the time-evolution of the overall conversion.

Average particles diameter

The average particles diameters are plotted versus the corresponding overall conversions in figure (2). Again, a good agreement is observed between experimental and simulated values. The curves show also that, for a same recipe smaller particles are produced when the temperature was increased.

On the other hand, in agreement with the results of Barudio et al. (1998), a slight effect of CTA concentration on the average particles diameters is also observed. If this slight effect of

CTA concentration, on both polymerization rate and average particles diameter exists, it can be explained in terms of desorbtion of chain transferred radicals from the polymer particles. But at the level of CTA concentrations used in these experiments, this effect could also be considered as the result of run-to-run poor reproducibility. This phenomenon be will be investigated in the validation in batch conditions (subsection 4.3.1).
Moreover, the coagulation of the particles was not observed under the experimental conditions used in this work (high concentrations of surfactant and adapted stirring). On the other hand the time-evolution of the average particles diameters (both experimental and simulated) showed that these diameters increase regularly and no coagulation was observed during the different stages of the process.

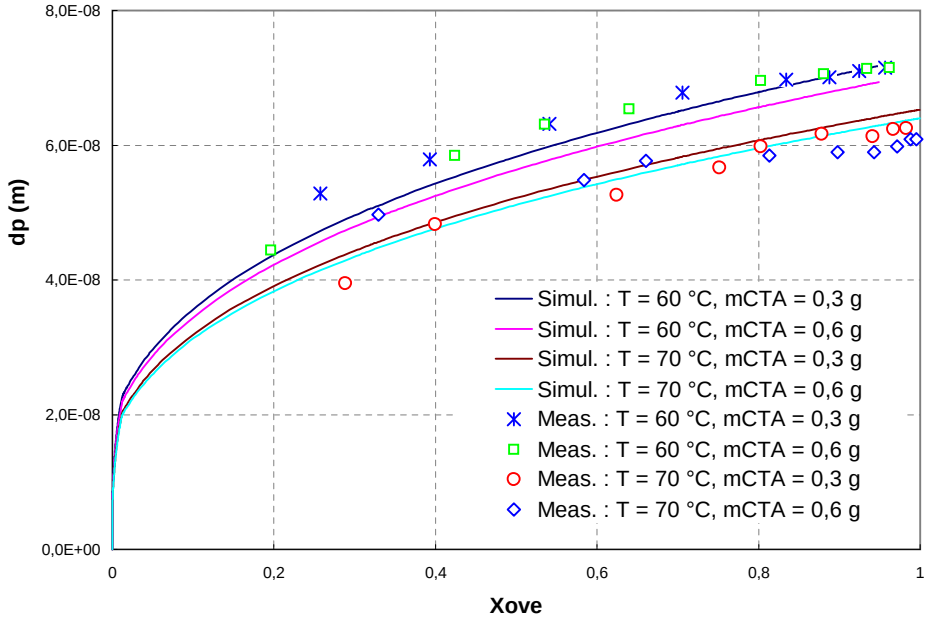

Figure 2: Effect of concentration of CTA and reaction temperature on the average particles diameter.

Number and weight average molecular weights
Figures (3) and (4) present the evolution of the number and weight average molecular weights ($\bar{M}_n$,$\bar{M}_w$) versus the overall conversion. In both cases we notice a good agreement between experimental and simulated values. Nevertheless the results of $\bar{M}_n$ seem to be more precise.

On the other hand, the results show that the general tendencies of radical polymerizations have been successfully modelled: an increase of temperature and of CTA concentration leads to a decrease of the average molecular weights.

Residual mass fraction of styrene
Figure 5 shows the time-evolution of the residual fraction of styrene. Due to the difference between the reactivity ratios of butyl acrylate and styrene, a slight drift is observed showing that the styrene consumption is favored.

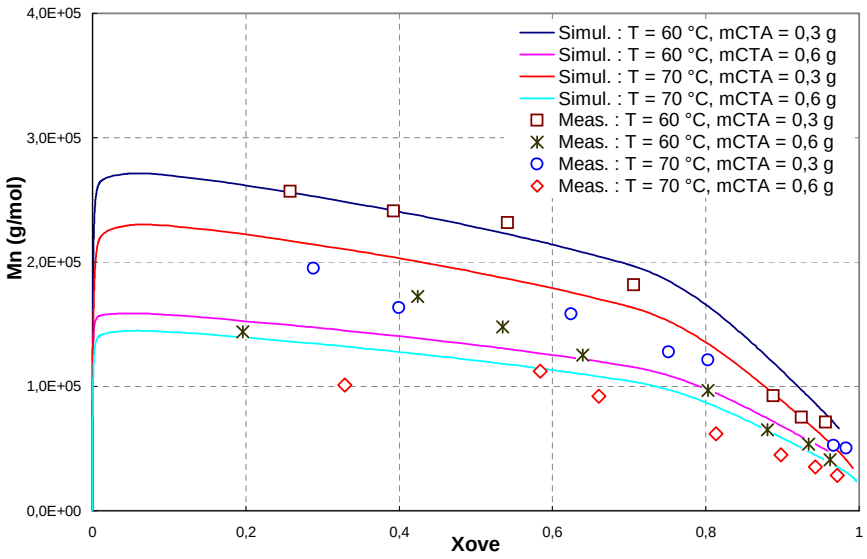

Figure 3: Effect of concentration of CTA and reaction temperature on the number average molecular weights.

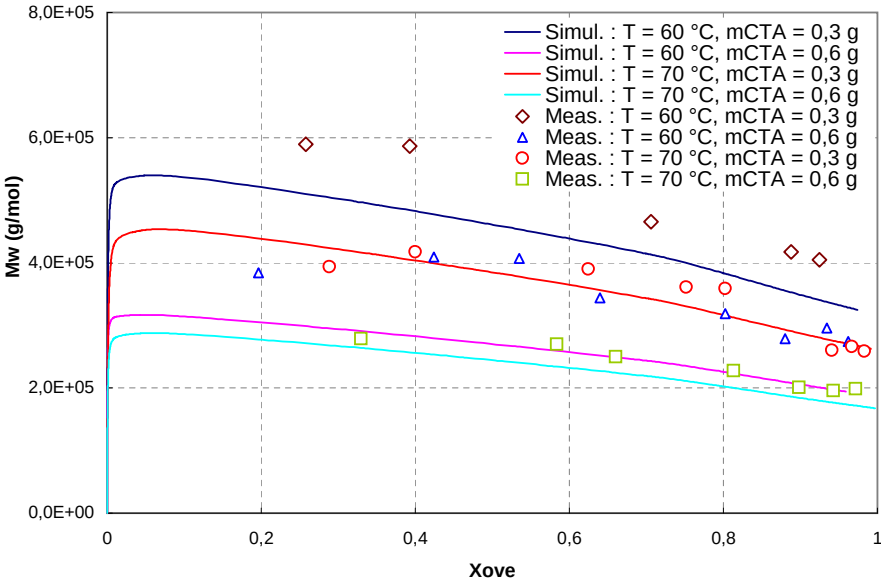

Figure 4: Effect of concentration of CTA and reaction temperature on the weight average molecular weights.

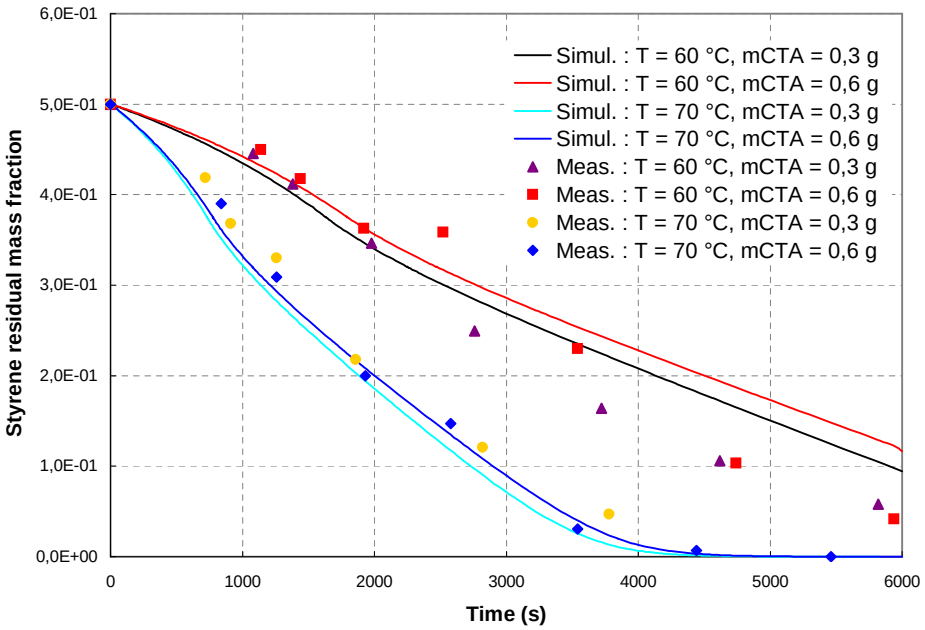

Figure 5: Effect of concentration of CTA and reaction temperature on the time-evolution of styrene residual mass fraction.

Globally all these results show an acceptable agreement between the model and the experiments.

4.3. Model validation

Several new experiments carried out in batch and fedbatch modes respectively, were used to validate the model.

4.3.1. Batch mode

The model was first validated using runs V1, V2 and V3 described (table (3)). Different concentrations of CTA were used to highlight the effect of this later on the polymerization kinetics.

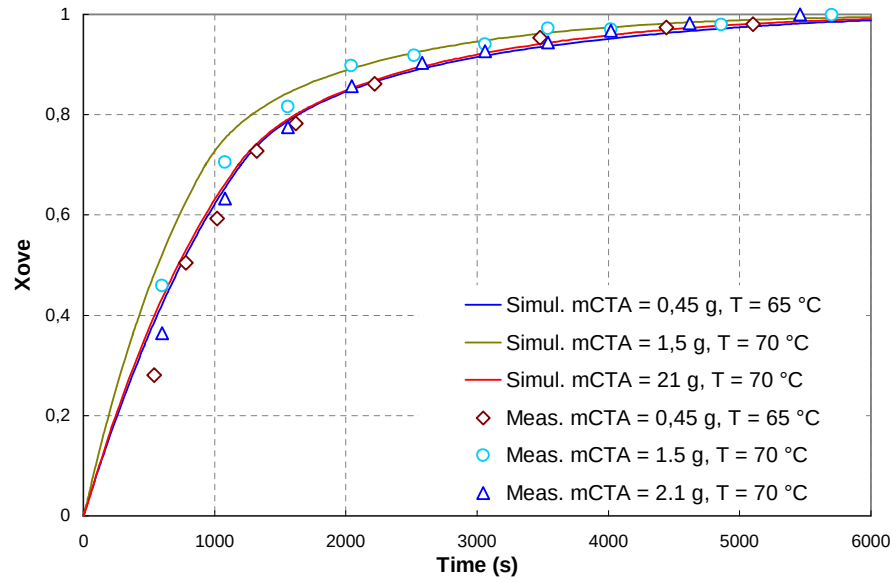

Figure 6: Validation of the model in the batch mode experiment: time-evolution of the overall conversion.

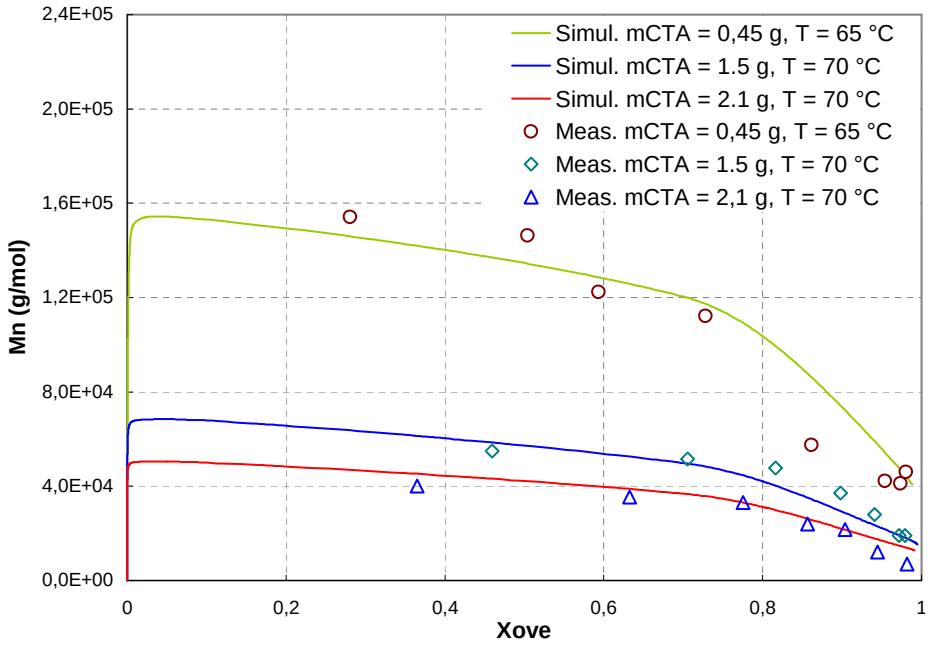

Figure 7: Validation of the model in the batch mode experiment: number average molecular weight versus overall conversion.

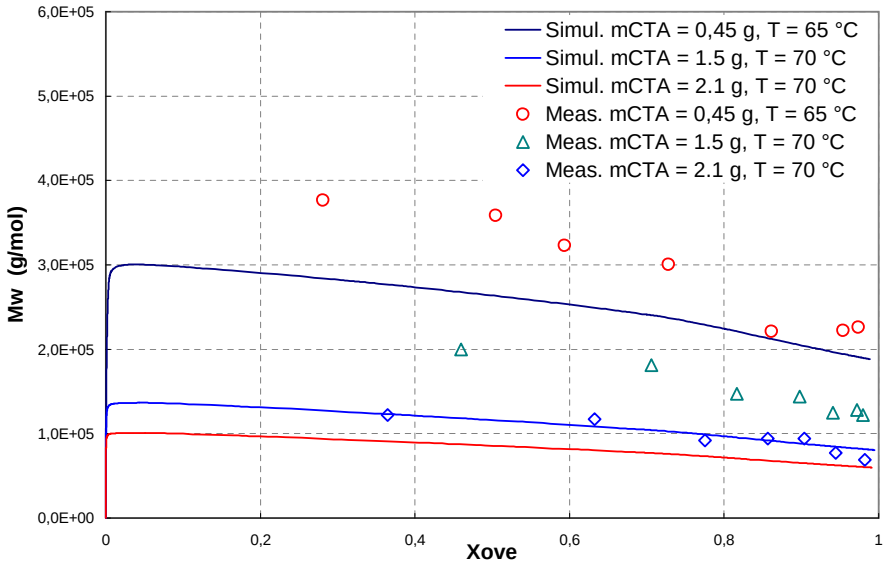

Figure 8: Validation of the model in the batch mode experiment: weight average molecular weight versus overall conversion.

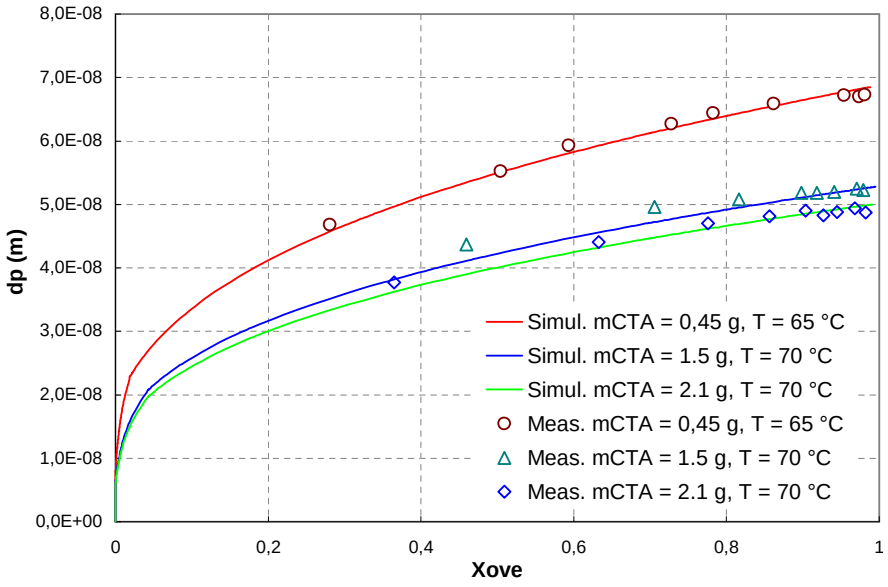

Figure 9: Validation of the model in the batch mode experiment: average particles diameter versus overall conversion.

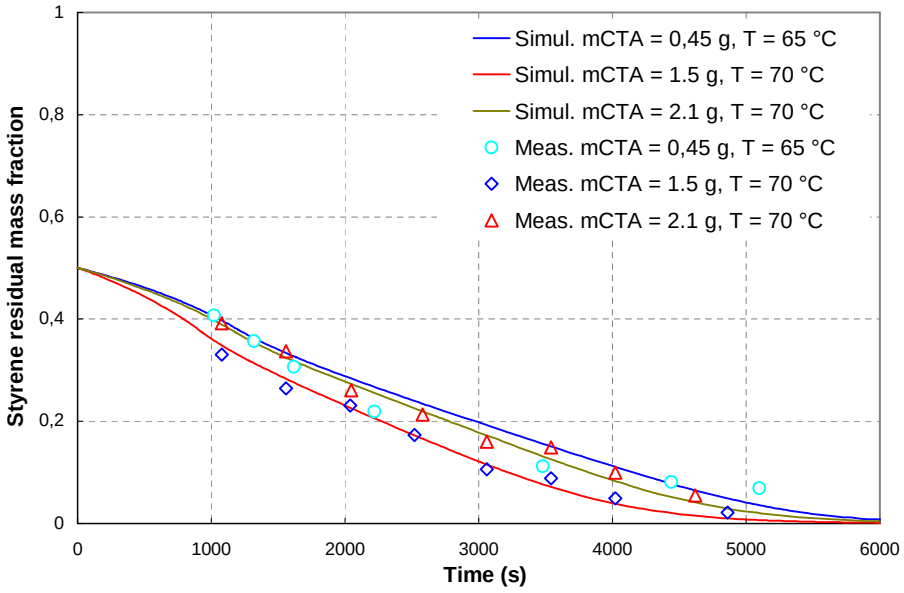

Figure 10: Validation of the model in the batch mode experiment: time-evolution of the styrene residual mass fraction.

Figures (6), (7), (8), (9), (10) make it possible to compare experimental and simulated results related to the overall conversion, number and weight average molecular weights, average particles diameters, and styrene residual mass fraction respectively. For each characteristic a fairly good agreement is still obtained between the model and the experiments.
On the other hand, figure (6) and (9) show that the conversion and the average particles diameters decrease as CTA concentration increases. These results are quite realistic since the desorption rate is affected by the CTA.

4.3.2. Fedbatch process

The operating conditions used for this run are given in table 4.
An initial charge, composed of the two monomers, water, surfactant and CTA (30 % of the total charge) was introduced into the reactor and brought to the desired reaction temperature under nitrogen atmosphere. The initiator was then added as a shot. After a batch pre-period of 18.5 minutes (seeding period), the remaining charge (preemulsion) was fed into the reactor according the feed profile given in figure 11.

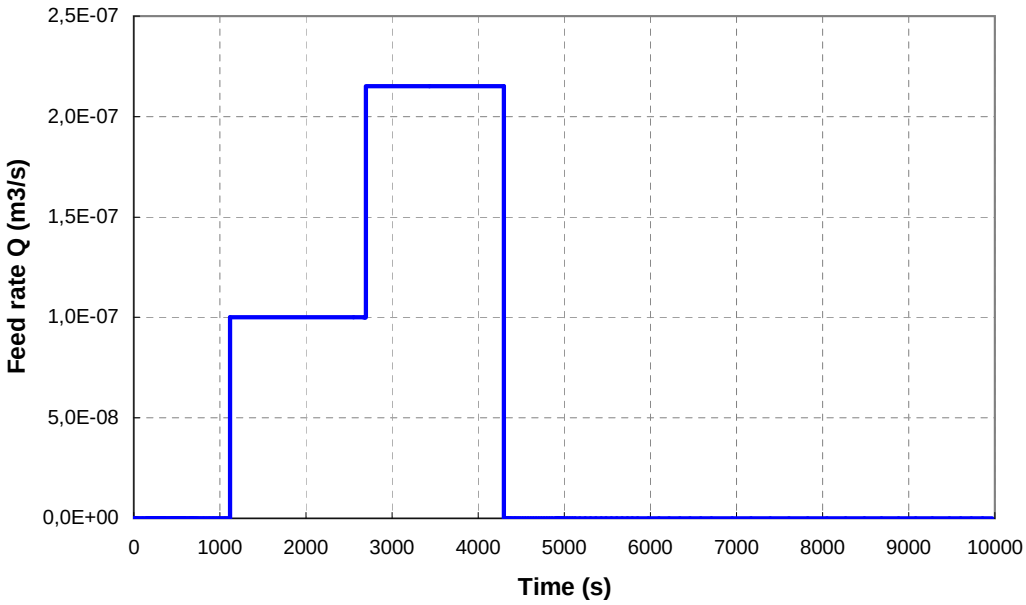

Figure 11: Feed rate profile used for the fedbatch run.

Figures 12 to 15 show again a fairly good agreement between experimental and simulated data and confirm the validity of the model.

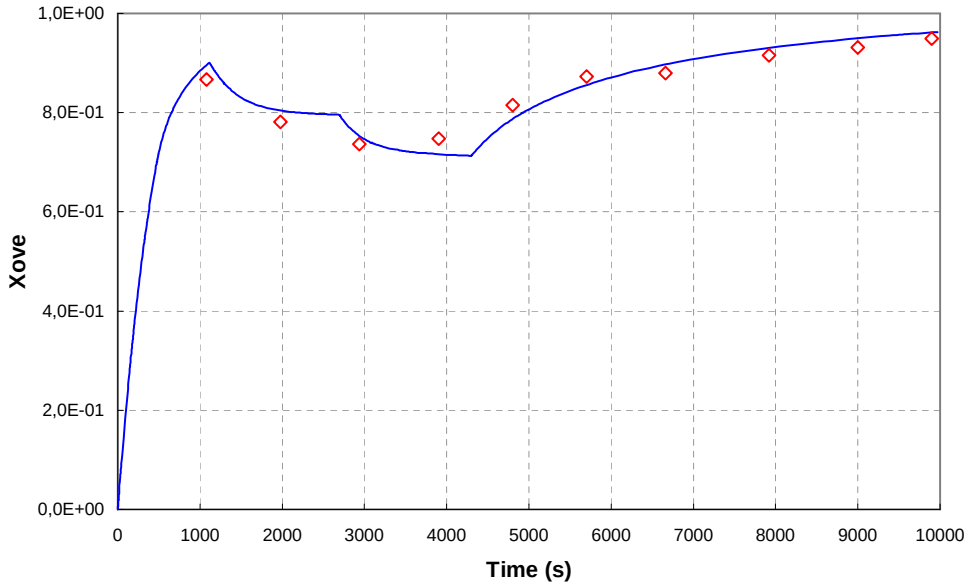

Figure 12: Validation of the model in the fedbatch mode experiment: time-evolution of the overall conversion.

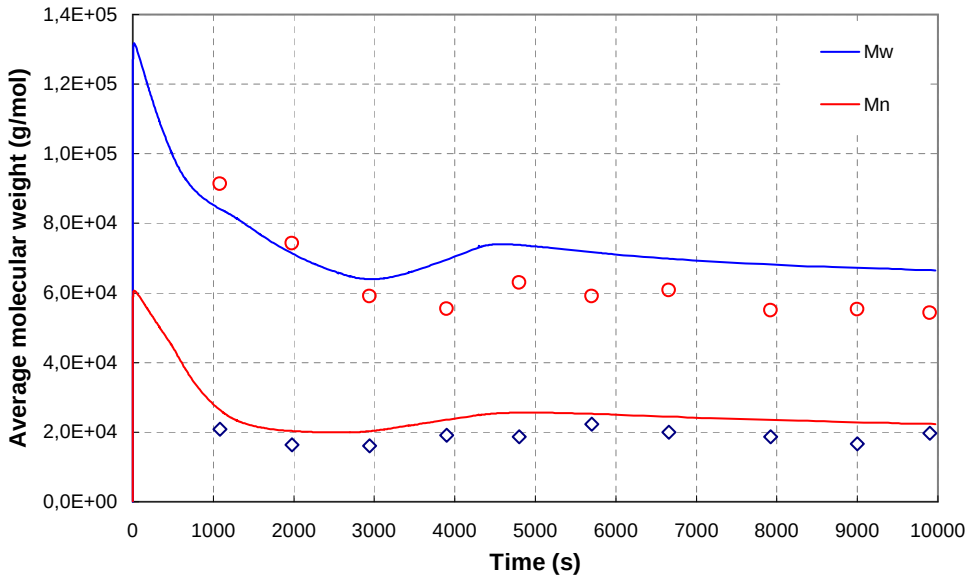

Figure 13: Validation of the model in the fedbatch mode experiment: time-evolution of the number and weight average molecular weights.

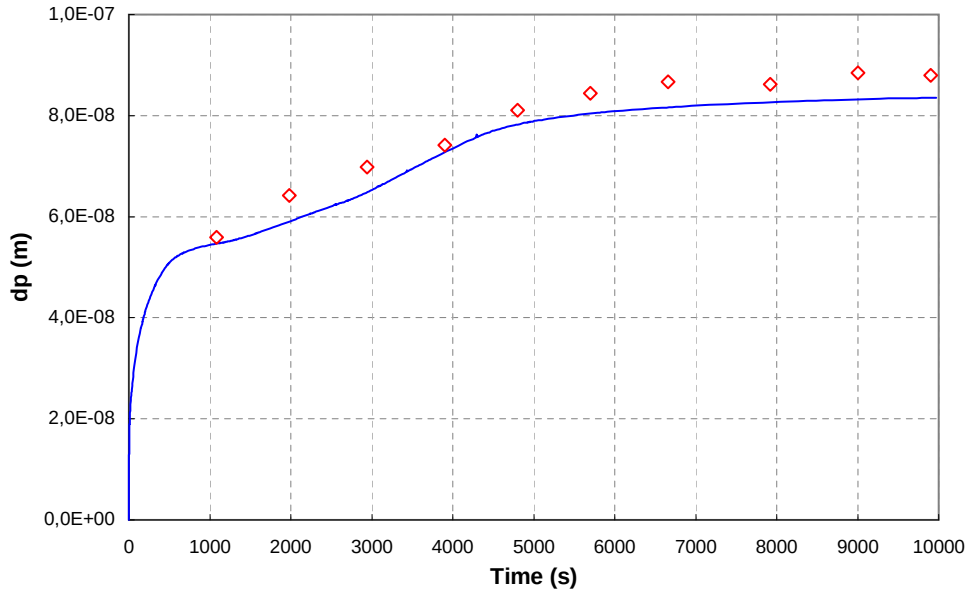

Figure 14: Validation of the model in the fedbatch mode experiment: time-evolution of the average particles diameters.

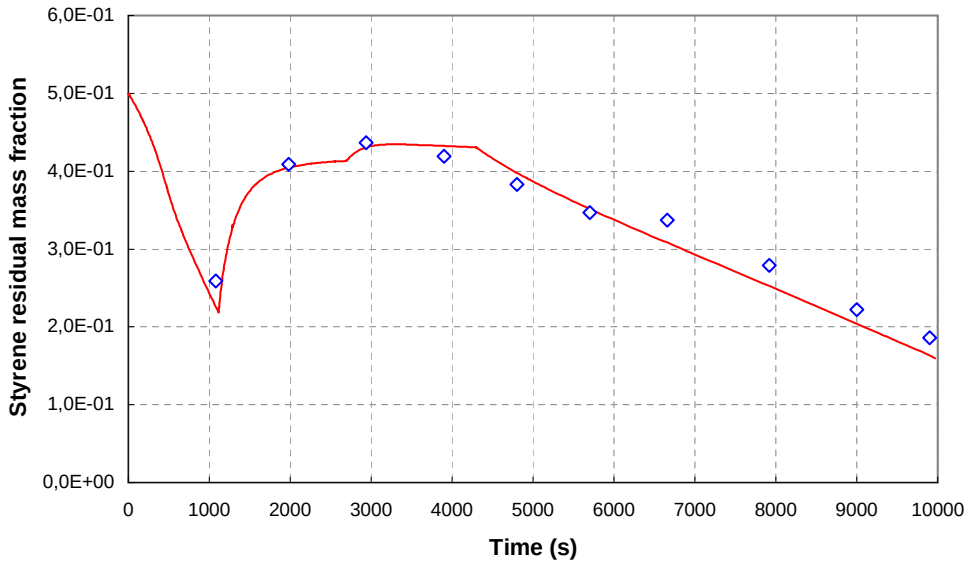

Figure 15: Validation of the model in the fedbatch mode experiment: time-evolution of the styrene residual mass fraction.

5. Conclusions

In this work, a dynamic reactor model was developed for the emulsion copolymerization of styrene and butyl acrylate in the presence of n-C12 mercaptan as chain transfer agent. This model is based on the kinetics of the complex elementary chemical reactions occurring both in the aqueous phase and in the particles. It takes into account the particles nucleation, the radicals absorption and desorption, and the partition of each monomer, CTA and inhibitor between the monomers droplets, the aqueous phase and the polymer particles. It considers also the gel and glass effects occurring during the copolymerization and the diffusion limitations of CTA from droplets to the aqueous phase whereas monomers are not subject to such limitations. The desorption rate which highlights the CTA effects is obtained by using the material balance on the oligoradicals and a constant value of the desorption coefficient. This approach is quite different from those proposed in literature where different expressions of the desorption coefficient are used according to the species used in the polymerization process.

A new approach was used to simplify the population balance by using two differential equations instead of the large number of differential equations generally used for the same purpose. This approach allowed reducing the corresponding simulation time.

21 parameters of the model were estimated by minimizing the errors between the predicted and the measured data using a stochastic optimization method based on a genetic algorithm, while 27 other were taken from literature.

The analysis of the associated results clearly showed that the agreement between the model predictions and experimental data is quite satisfactory.

The resulting model was then successfully validated through four additional polymerizations carried out under batch and fedbatch modes respectively. It is now able (i) to predict the global

monomers conversion, the residual monomers contents, the number and weight average molecular weights of the resulting copolymers as well as the average particles diameters, (ii) to study the effect of the concentration of the chain transfer agent on both polymerization rate and average molecular weights. This study showed also that the polymerization rate as well as the average particles diameter decreased as CTA concentration is increased.

Notations

A_d	total surface area of the droplets, m^2
A_p	total surface area of the particles, m^2
a	Flory adjustment parameter, $K \cdot kg \cdot kmol^{-1}$
a_e	surfactant molecular area at $50°C$, nm^2
a_S	surface covered by one kmole of surfactant, $m^2 \cdot kmol^{-1}$
b^{ge}	gel coefficient of termination reaction
b^{gl}	glass coefficient of termination reaction
d_d	average droplets diameter, m
d_{mic}	average micelles diameter, m
d_p	average particles diameter, m
D_{pi}	diffusion coefficient of the free radicals i in the particles, $m^2 \cdot s^{-1}$
D_{wi}	diffusion coefficient of the free radicals i in the aqueous phase, $m^2 \cdot s^{-1}$
E_d	activation energy of the initiator, $J \cdot mol^{-1}$
E_e	thermal expansion factor of a surfactant molecule, K
E_{p11}	activation energy of butyl acrylate propagation, $J \cdot mol^{-1}$
E_{p22}	activation energy of styrene propagation, $J \cdot mol^{-1}$
E_{t11}	activation energy of butyl acrylate termination reaction, $J \cdot mol^{-1}$
E_{t22}	activation energy of styrene termination reaction, $J \cdot mol^{-1}$
E_{trm11}	activation energy of butyl acrylate monomer transfer, $J \cdot mol^{-1}$
E_{trm22}	activation energy of styrene monomer transfer, $J \cdot mol^{-1}$
f	efficiency factor of initiator decomposition
f_{aqi}	fraction of radicals i in the aqueous phase
f_b	fraction of styrene in the reactor
f_{0i}	initial molar fraction of monomer i in the reactor
F_i	residual mass fraction of monomer i
h	number of free radicals in particular particle
I	total number of moles of initiator in the aqueous phase, $kmol$
K_{di}	partition coefficient of monomer i between the droplets and the aqueous phase
K_{dTA}	partition coefficient of the chain transfer agent between the droplets and the aqueous phase
K_{dZ}	partition coefficient of the inhibitor between the droplets and the aqueous phase
K_{pi}	partition coefficient of monomer i between the aqueous phase and the particles
K_{pTA}	partition coefficient of the chain transfer agent between the aqueous phase and the particles
K_{pZ}	partition coefficient of the inhibitor between the aqueous phase and the particles
k_{cpi}	capture rate coefficient of free radicals i, $m^2 \cdot kmol^{-1} \cdot s^{-1}$
k_d	initiator decomposition constant, s^{-1}
k_{desi}	desorption rate coefficient of the radical ended by a monomer i, $m^2 \cdot kmol^{-1} \cdot s^{-1}$

k_i	transfer coefficient of free radicals formed by one monomer unit i, $m \cdot s^{-1}$
k_N	nucleation rate coefficient, $m^2 \cdot kmol^{-1} \cdot s^{-1}$
k_{pij}	propagation rate coefficient of monomer j with a free radical ended by i, $m^3 \cdot kmol^{-1} \cdot s^{-1}$
$k_{TA,dw}$	mass transfer coefficient of the CTA between droplets and aqueous phase, $m \cdot s^{-1}$
k_{TApi}	transfer coefficient chain transfer agent to radical i in particles, $m^3 \cdot kmol^{-1} \cdot s^{-1}$
k_{tij}	termination rate coefficient (radical ended by i- radical ended by j), $m^3 \cdot kmol^{-1} \cdot s^{-1}$
k_{trmij}	transfer to monomer rate coefficient (radical ended by i- monomer j), $m^3 \cdot kmol^{-1} \cdot s^{-1}$
k_{Zpi}	inhibition rate coefficient of radicals i in the particles, $m^3 \cdot kmol^{-1} \cdot s^{-1}$
k_{Zaq}	inhibition rate coefficient in the aqueous phase, $m^3 \cdot kmol^{-1} \cdot s^{-1}$
L_k	k^{th} normalised moment of the macromolecules
M_i	total number of moles of residual monomer i, $kmol$
M_p^i	total number of moles of monomer i in the particles, $kmol$
M_{pi}	total mole number of monomer i in the particles, $kmol$
M_{Ti}	total number of moles of monomer i introduced in the reactor (initial and fed to the reactor), $kmol$
M_M^i	molecular weight of the monomer i, $kg \cdot kmol^{-1}$
M_M^Z	molecular weight of the inhibitor, $kg \cdot kmol^{-1}$
M_M^{TA}	molecular weight of the chain transfer agent, $kg \cdot kmol^{-1}$
$\bar{M}_n$	number average molecular weight, $kg \cdot kmol^{-1}$
$\bar{M}_w$	weight average molecular weight, $kg \cdot kmol^{-1}$
m_{di}	equilibrium constant of free radicals ended by i between aqueous and particle phases
N_A	Avogadro number, $kmol^{-1}$
N_m	total number of macromolecules, $kmol$
N_{mic}	total number of moles of micelles (number of micelles/N_A), $kmol$
N_p	total number of moles of particles (number of particles/N_A), $kmol$
$\bar{n}$	average number of free radicals in a particle
$\tilde{n}$	average number of pairs of free radicals in a particle
n_s	number of surfactant molecules per micelle
P_i	fraction of free radicals ended by a monomer unit i in the particles
Q_f	total feed rate of monomers, inhibitor, transfer agent and surfactant, $m^3 \cdot s^{-1}$
Q_{If}	feed rate of initiator, $m^3 \cdot s^{-1}$
R_{aq}	the number of moles of free radicals in the aqueous phase, $kmol$
R_{pi}	the number of moles of free radicals i in the particles, $kmol$
$\mathcal{R}_d$	thermal decomposition rate of initiator in the aqueous phase, $kmol \cdot s^{-1}$
$\mathcal{R}_N$	total micellar nucleation rate, $kmol \cdot s^{-1}$
$\mathcal{R}_p$	total propagation rate , $kmol \cdot s^{-1}$
$\mathcal{R}_{TAp}$	chain transfer agent consumption rate in particles, $kmol \cdot s^{-1}$
$\mathcal{R}_T$	total termination rate, $kmol \cdot s^{-1}$
$\mathcal{R}_{TC}$	total termination rate by combination, $kmol \cdot s^{-1}$
$\mathcal{R}_{TD}$	total termination rate by disproportionation, $kmol \cdot s^{-1}$
$\mathcal{R}_{trm}$	total transfer to monomer rate, $kmol \cdot s^{-1}$
$\mathcal{R}_{Zaq}$	inhibitor consumption rate in the aqueous phase, $kmol \cdot s^{-1}$
$\mathcal{R}_{Zp}$	inhibitor consumption rate in particles, $kmol \cdot s^{-1}$
$\mathcal{R}_{Zpi}$	inhibitor consumption rate in particles with free radicals ended by i, $kmol \cdot s^{-1}$

$\mathcal{S}_{aq}$	number of moles of surfactant in the aqueous phase, *kmol*
$\mathcal{S}$	total number of moles of surfactant in the reactor, *kmol*
$\mathcal{S}_d$	number of moles of surfactant on the droplets, *kmol*
$\mathcal{S}_p$	number of moles of surfactant on particles, *kmol*
$\mathcal{S}_{mic}$	number of moles of surfactant in the micelles, *kmol*
X_{ove}	overall mass conversion
$[CTA]_f$	concentration of the transfer agent in the feed, $kmol \cdot m^{-3}$
$[I]_f$	concentration of the initiator in the feed, $kmol \cdot m^{-3}$
$[M_i]_f$	concentration of monomer i in the feed, $kmol \cdot m^{-3}$
$[S]_f$	concentration of the surfactant in the feed, $kmol \cdot m^{-3}$
$[Z]_f$	concentration of the inhibitor in the feed, $kmol \cdot m^{-3}$

Greek letters

ω_i	fraction of radicals ended by monomer i formed only by one monomer unit
δ	overall ratio of nucleation and capture rate coefficients
δ_i	ratio of nucleation and capture coefficients due to monomer unit i
δ_{mi}	ratio of transfer resistance in aqueous phase on overall transfer resistance of free radicals ended by a monomer unit i
τ	ratio of the termination rates by disproportionation and combination
ρ_i	density of the monomer i, $kg \cdot m^{-3}$
ρ_{pi}	density of the homopolymer i, $kg \cdot m^{-3}$
ρ_Z	density of the inhibitor, $kg \cdot m^{-3}$
ρ_{TA}	density of the chain transfer agent, $kg \cdot m^{-3}$
σ	coefficient related to the saturation degree of the particle
λ_k	k^{th} normalized moment of the macroradicals
$\bar{w}_j$	fraction of macroradicals with a degree of polymerization j
w_j	fraction of macromolecules with a degree of polymerization j
χ_i	fraction of radicals i formed by one unit of the monomer i in the particles

References

Alhamad, B., Romagnoli, J., Gomes, V., 2005. Advanced modelling and optimal operating strategy in emulsion copolymerization: Application to styrene/ mma system. Chemical Engineering Science. 60, 2795–2813.

Arzamendi, G., De la Cal, J. C., Asua, J. M., 1992. Optimal monomer addition policies for composition control of emulsion terpolymers. Angewandte Makromolekulare Chemie. 194, 47–64.

Asua, J. M., 2004. Emulsion polymerization: From fundamental mechanisms to process developments. Journal of Polymer Science. 42, 1025–1041.

Barudio, I., Guillot, J., Fevotte, G., 1998. Efficiency of mercaptan chain transfer agents in emulsion copolymerizations. 1. influence on kinetics and microstructure. modeling of radical desorption. Journal of Polymer Science. 36, 157–168.

Baillagou, P. E. and Soong, D. S., 1985. Molecular weight distribution of products of free radical nonisothermal polymerization with gel effect. Simulation for polymerization of poly(methyl methacrylate). Chemical Engineering Science.40, 87–104.

Chern, C. S., 2006. Emulsion polymerization mechanisms and kinetics. Progress in Polymer Science. 31, 443–486.

Dube, M. A., Penlidis, A., 1996. Mathematical modeling of emulsion copolymerization of acrylonitrile/butadiene. Industrial and Engineering Chemistry Research. 35, 4434–4448.

Dube, M. A., Soares, J. B. P., Penlidis, A., Hamielec, A. E., 1997. Mathematical modeling of multicomponent chain-growth polymerization in batch, semi-batch and continuous reactors: A review. Industrial and Engineering Chemistry Research. 36, 966–1015.

Frank, R. L., Smith, P. V., Woodward, F. E., Reynolds, W. B., Canterino, P. J., 1948. Mercaptan structure and regulator activity in emulsion polymerizations. Journal of Polymer Science. 3, 39–49.
Gao, J., Penlidis, A., 2002. Mathematical modeling and computer simulator/database for emulsion polymerizations. Progress in Polymer Science. 27, 403–535.
Gilbert, R. G. (Ed.), 1995. Emulsion polymerization. A mechanistic approach. New York: Academic Press.
Ginsburger, E., Pla, F., Fonteix, C., Hoppe, H., Massebeuf, S., Hobbes, P., Swaels, P., 2003. Modelling and simulation of batch and semi-batch emulsion copolymerization of styrene and butyl acrylate. Chemical Engineering Science. 58, 4493–4514.
Gugliotta, L. M., Arzamendi, G., Asua, J. M., 1995. monomer partition model in mathematical modeling of emulsion copolymerization systems. Journal of Applied Polymer Science. 55, 1017–1039.
Harkins, W. D., 1947. Theory of the mechanism of emulsion polymerization. Journal of the American Chemical Society. 69, 1428–1444.
Hoppe, S., Schrauwen, C., Fonteix, C., Pla, F., 2005. Modeling of the emulsion terpolymerization of styrene, a-methylstyrene and methyl methacrylate. Macromolecular Materials and Engineering. 290, 384–403.
Kolthoff, I. M., Harris, W. E., 1947. Mercaptans as promoters and modifiers in emulsion copolymerization of butadiene and styrene using potassium persulfate as catalyst. ii. mercaptans as modifiers. Journal of Polymer Science. 2, 49–71.
Lewis, W. K., Whitman, W. G., 1924. Principles of gas absorption. Industrial Engineering Chemistry. 16, 1215–1220.
Martinet, F., 1992. Etude et modélisation du greffage de mélanges -méthylstyrène / méthacryalyte de méthyle sur des semences de polybutadiène comme modification des mbs. Ph.D. thesis, Université Claude Bernard, Lyon 1, France.
Mendoza, J., De la Cal, J., Asua, M. A., 2000. Kinetics of the styrene emulsion polymerization using n-dodecyl mercaptan as chain-transfer agent. Journal of Polymer Science: Polymer Chemistry. 38, 4490–4505.
Nomura, M., 1982. Desorption and reabsorption of free radicals in emulsion polymerization. In: Piirma, I. (Ed.), Emulsion polymerization. New York: Academic Press., pp. 191–219.
Nomura, M., Harada, M., 1981. Rate coefficient for radical desorption in emulsion polymerization. Journal of Applied Polymer Science. 26, 17–26.
Nomura, M., Minamino, Y., Fujita, K., Harada, M., 1982. The role of chain transfer agent in emulsion polymeriztion of styrene. Journal of Polymer Science: Pol. Chem. 20. pp. 1261–1270.
Nomura, M., Suzuki, H., Tokunaga, H., Fujita, K., 1994. Mass transfer effects in emulsion polymerization systems. i. diffusional behaviour of chain transfer agents in the emulsion polymerization of styrene. Journal of Applied Polymer Science. 51, 21–23.
Rawlings, J. B., Ray, W. H., 1988. The modeling of batch and continuous emulsion polymerization reactors. part i. model formulation and sensitivity to parameters. Polymer Engineering and Science. 28(5), 237–255.
Salazar, A., Gugliotta, L. M., Vega, J. R., Meira, G. R., 1998. Molecular weight control in a starved emulsion polymerization of styrene. Industrial and Engineering Chemistry Research. 37 (9), 3582–3591.
Sgard, A., 2000. Modélisation de procédés discontinus et semi-continus de polymérisation en émulsion. Ph.D. thesis, INPL, Nancy, France.
Smith, W. V., 1946a. Regulator theory in emulsion polymerization. ii. control of reaction rate by diffusion for high molecular weight mercaptans. Journal of American Chemical Society. 68, 2064–2069.
Smith, W. V., 1946b. Regulator theory in emulsion polymerization.1 i. chain transfer of low molecular weight mercaptans in emulsion and oil-phase. Journal of American Chemical Society. 68, 2059–2064.
Storti, G., Carra, S., Morbidelli, M., 1989. Kinetics of multimonomer emulsion polymerization: The pseudo-homopolymerization approach. Journal of Applied Polymer Science, 37, 2443–2467.
Thickett, S., Gilbert, R. G., 2007. Emulsion polymerization: State of the art in kinetics and mechanisms. Polymer. 48, 6965–6991.
Villermaux, J., Blavier, L., 1984. Free radical polymerization engineering. i. a new method for modeling free radical homogeneous polymerization reactions. Chemical Engineering Science. 39(1), 87–99.
Walter, E., Pronzato, L. (Eds.), 1994. Identification de modeles parametriques à partir de données experimentales. Paris, Masson.

Appendix A: Partition of the different species

The total volume of the aqueous phase :

$$V_{aq} = V_{eau} + V_{aq}^{1} + V_{aq}^{2} + V_{aq}^{Z} + V_{aq}^{CTA} \tag{.1}$$

The total volume of the particules :

$$V_p = V_{pol} + V_p^1 + V_p^2 + V_p^Z + V_p^{CTA} \tag{.2}$$

The total volume of the droplets :

$$V_d = V_d^1 + V_d^2 + V_d^Z + V_d^{CTA} \tag{.3}$$

The total volume engaged in the reactor :

$$V_R = V_{aq} + V_p + V_d \tag{.4}$$

The partion coefficients of specie i (i = 1, 2, Z, CTA) between the different phases are defined as follows (Gugliotta et al. (1995))

$$K_{di} = \frac{V_d^i / V_d}{V_{aq}^i / V_{aq}} \tag{.5}$$

$$K_{pi} = \frac{V_{aq}^i / V_{aq}}{V_p^i / V_p} \tag{.6}$$

$$K_{pi} K_{di} = \sigma_i \tag{.7}$$

Where K_{di} partition coefficient of i between the droplets and the aqueous phase, K_{pi} the partition coefficient of i between the aqueous phase and the particles. σ_i a coefficient related to the saturation degree of the particle (partition coefficient of the i between the droplets and the particles.
According to Arzamendi et al. (1992), we assume that all species have the same value of the partition coeffiecient droplets and particles ($\sigma_i = \sigma$).
Equations .5, .7 lead to the fraction of i in the droplets,

$$\frac{V_d^i}{V_d} = K_{di} \frac{V_{aq}^i}{V_{aq}} = \sigma \frac{V_p^i}{V_p} \tag{.8}$$

The sum of the fraction of all species gives,

$$\frac{V_d^1}{V_d} + \frac{V_d^2}{V_d} + \frac{V_d^Z}{V_d} + \frac{V_d^{CTA}}{V_d} = \sigma \left(\frac{V_p^1}{V_p} + \frac{V_p^2}{V_p} + \frac{V_p^Z}{V_p} + \frac{V_p^{CTA}}{V_p} \right)$$

By using equations .2 and .3 we get

$$1 = \sigma \left(\frac{V_p - V_{pol}}{V_p} \right) \tag{.9}$$

$$V_p = \left(\frac{\sigma}{\sigma - 1} \right) V_{pol} \tag{.10}$$

On the other hand, we can write the total volume of each specie i (M_1, M_2, Z, CTA) in the reactor as follows

$$V_i = M_i \frac{M_M^i}{\rho_i} = V_d^i + V_p^i + V_{aq}^i \tag{.11}$$

From equations .6 and .7 we get the volume of i in the droplets and the aqueous phase :

$$V_d^i = \frac{V_p^i V_d \sigma}{V_p} \tag{.12}$$

$$V_{aq}^i = \frac{V_p^i V_{aq} K_{pi}}{V_p} \tag{.13}$$

Hence, the total volume of i and the fraction of i in the particle are as follows:

$$V_i = \frac{V_p^i}{V_p}\left(V_p + V_d\sigma + V_{aq}K_{pi}\right) = M_i \frac{M_M^i}{\rho_i} \tag{.14}$$

$$\frac{V_p^i}{V_p} = \frac{M_i M_M^i}{\rho_i\left(V_p + V_d\sigma + V_{aq}K_{pi}\right)} \tag{.15}$$

As a first approach, the total number of moles of monomer i in the particles is given by,

$$M_{pi} = \frac{V_p^i \rho_i}{M_M^i} \tag{.16}$$

By using equation .15 we get the final expressions of the number of moles for the monomers, inhibitor and CTA in the particles

$$M_{pi} = \frac{M_i V_p}{\left(V_p + V_d\sigma + V_{aq}K_{pi}\right)} \tag{.17}$$

$$\begin{aligned} Z_p &= \frac{V_p^Z \rho_Z}{Z} \\ &= \frac{Z V_p}{\left(V_p + V_d\sigma + V_{aq}K_{pZ}\right)} \end{aligned} \tag{.18}$$

For the CTA the number of moles in the particles supposed in equilibrium is as follows (for the real number see Appendix 5)

$$
\begin{aligned}
CTA_p^e &= \frac{V_p^{CTA}\rho_{CTA}}{CTA} \\
&= \frac{CTA\ V_p}{\left(V_p + V_d\sigma + V_{aq}K_{pTA}\right)}
\end{aligned} \tag{.19}
$$

In the same way, we get the final expressions of the number of moles for the monomers and the inhibitor in the aqueous phase and the molar fraction of monomer i in the aqueous phase,

$$
M_{aqi} = K_{pi}M_{pi}\frac{V_{aq}}{V_p} \tag{.20}
$$

$$
Z_{aq} = K_{pz}Z_p\frac{V_{aq}}{V_p} \tag{.21}
$$

$$
f_{aqi} = \frac{\frac{V_{aq}^1\rho_i}{M_M^i}}{\sum\limits_{j=1,2}\frac{V_{aq}^1\rho_j}{M_M^j}} \tag{.22}
$$

$$
= \frac{K_{pi}M_{pi}}{\sum\limits_{j=1,2}K_{pj}M_{pj}} \tag{.23}
$$

Appendix B: CTA concentration in the particles

As a consequence of the transfer limitation of the CTA from droplets to the aqueous phase, the concentration in particles may be below the thermodynamic concentration. Salazar et al. (1998) derived an expression for a polymerization process under the same conditions. Accordingly we can derive the real concentration (moles number) of the CTA in the particles for the copolymerization process.
The partition coefficients under equilibrium conditions are,

$$
K_{dTA} = \frac{V_d^{CTA}/V_d}{V_{aq}^{CTA}/V_{aq}} = \frac{[CTA]_d^e}{[CTA]_{aq}^e} \tag{.24}
$$

$$
K_{pTA} = \frac{V_{aq}^{CTA}/V_{aq}}{V_p^{CTA}/V_p} = \frac{[CTA]_{aq}^e}{[CTA]_p^e} \tag{.25}
$$

$$
K_{pTA}K_{dTA} = \frac{[CTA]_d^e}{[CTA]_p^e} \tag{.26}
$$

Under steady-state assumptions, the CTA's flow across the droplets-aqueous phase interface must be equal to the consumption by transfer to CTA in the polymer particles, and therefore

$$
\begin{aligned}
& k_{TA,dw} A_d \left([CTA]^i_{aq} - [CTA]_{aq} \right) \\
= \quad & k_{TA1} \frac{CTA_p}{V_p} R_{p1} + k_{TA2} \frac{CTA_p}{V_p} R_{p2} \\
= \quad & [CTA]_p \left(k_{TA1} R_{p1} + k_{TA2} R_{p2} \right)
\end{aligned} \tag{.27}
$$

where $k_{TA,dw}$ is the mass transfer coefficient of the CTA in the droplets-aqueous phase interface.
Assuming an equilibrium partition at the interfaces, we get

$$
K_{dTA} = \frac{[CTA]^i_d}{[CTA]^i_{aq}} \cong \frac{[CTA]_d}{[CTA]^i_{aq}} \tag{.28}
$$

and

$$
[CTA]^i_{aq} = \frac{[CTA]_d}{K_{dTA}} \tag{.29}
$$

$$
[CTA]_d \cong [CTA]^e_d = [CTA]^e_p K_{pTA} K_{dTA} \tag{.30}
$$

$$
\begin{aligned}
& k_{TA,dw} A_d \left([CTA]^e_p K_{pTA} - [CTA]_p K_{pTA} \right) \\
& \qquad = [CTA]_p \left(k_{TA1} R_{p1} + k_{TA2} R_{p2} \right)
\end{aligned} \tag{.31}
$$

By combining the different equations we finally get the real concentration and the moles number of the CTA in the particles

$$
[CTA]_p = \frac{[CTA]^e_p}{1 + \dfrac{k_{TA1} R_{p1} + k_{TA2} R_{p2}}{k_{TA,dw} A_d K_{pTA}}} \tag{.32}
$$

$$
CTA_p = \frac{CTA^e_p}{1 + \dfrac{k_{TA1} R_{p1} + k_{TA2} R_{p2}}{k_{TA,dw} A_d K_{pTA}}} \tag{.33}
$$

Appendix C: Population balance

The population balance equations of the particles containing $0, 1, \ldots i$ radical are given as follows

$$
\frac{d\left(N_P \upsilon_0\right)}{dt} = -\mathcal{R}_{cp} \upsilon_0 + \frac{\mathcal{R}_T}{\tilde{n}} \upsilon_2 + \left(\mathcal{R}_{Zp} + \mathcal{R}_{des} \right) \frac{\upsilon_1}{\bar{n}} \tag{.34}
$$

$$\begin{aligned}\frac{d\left(N_P \upsilon_1\right)}{dt} &= \mathcal{R}_N + 3\frac{\mathcal{R}_T}{\tilde{n}}\upsilon_3 - \mathcal{R}_{cp}\upsilon_1 + \mathcal{R}_{cp}\upsilon_0 \\ &+ \left(\mathcal{R}_{Zp} + \mathcal{R}_{des}\right)\frac{\left(2\upsilon_2 - \upsilon_1\right)}{\bar{n}} \end{aligned} \tag{.35}$$

$$\begin{aligned}\frac{d\left(N_P \upsilon_i\right)}{dt} &= \mathcal{R}_{cp}\left(\upsilon_{i-1} - \upsilon_i\right) \\ &+ \frac{\mathcal{R}_T}{2\tilde{n}}\left(\left(i+2\right)\left(i+1\right)\upsilon_{i+2} - i\left(i-1\right)\upsilon_i\right) \\ &+ \left(\mathcal{R}_{Zp} + \mathcal{R}_{des}\right)\frac{\left(\left(i+1\right)\upsilon_{i+1} - i\upsilon_i\right)}{\bar{n}} \end{aligned} \tag{.36}$$

such as

$$\sum_{i=0}^{\infty} \upsilon_i = 1$$

$$\sum_{i=0}^{\infty} i\upsilon_i = \sum_{i=1}^{\infty} i\upsilon_i = \bar{n}$$

By multiplying the equations (.34, .35, .36) by i, the sum gives :

$$\begin{aligned}\frac{d\left(N_P \bar{n}\right)}{dt} &= \mathcal{R}_N + \mathcal{R}_{cp}\left(\sum_{i=1}^{\infty} i\upsilon_{i-1} - \bar{n}\right) \\ &+ \frac{\mathcal{R}_T}{2\tilde{n}}\left(\sum_{i=0:1}^{\infty} i\left(i+1\right)\left(i+2\right)\upsilon_{i+2} - \sum_{i=1:2}^{\infty} i^2\left(i-1\right)\upsilon_i\right) \\ &+ \frac{\left(\mathcal{R}_{Zp} + \mathcal{R}_{des}\right)}{\bar{n}}\left(\sum_{i=0:1}^{\infty} i\left(i+1\right)\upsilon_{i+1} - \sum_{i=1:2}^{\infty} i^2\upsilon_i\right) \end{aligned} \tag{.37}$$

All terms of the equation .37 could be simplified as follows,

$$\sum_{i=1}^{\infty} i\upsilon_{i-1} = \sum_{j=0}^{\infty}\left(j+1\right)\upsilon_j = \bar{n} + 1$$

$$\begin{aligned}&\sum_{i=0}^{\infty} i\left(i+1\right)\left(i+2\right)\upsilon_{i+2} - \sum_{i=2}^{\infty} i^2\left(i-1\right)\upsilon_i \\ &= -2\sum_{j=2}^{\infty} j\left(j-1\right)\upsilon_j = -2\tilde{n}\end{aligned}$$

$$\begin{aligned}\sum_{i=0}^{\infty} i\left(i+1\right)\upsilon_{i+1} - \sum_{i=1}^{\infty} i^2\upsilon_i &= \sum_{j=2}^{\infty}\left(j\left(j-1\right) - j^2\right)\upsilon_j \\ &= -\bar{n}\end{aligned}$$

Finally, the equation .37 becomes,

$$\begin{aligned}\frac{d\left(N_P\tilde{n}\right)}{dt} &= \mathcal{R}_N + \mathcal{R}_{cp} + \frac{\mathcal{R}_T}{2\tilde{n}}\left(-2\tilde{n}\right) - \left(\mathcal{R}_{Zp} + \mathcal{R}_{des}\right) \\ &= \mathcal{R}_N + \mathcal{R}_{cp} - \left(\mathcal{R}_T + \mathcal{R}_{Zp} + \mathcal{R}_{des}\right) \end{aligned} \tag{.38}$$

In the same way, by multiplying the equations (.34, .35, .36) by $i(i-1)$, the sum gives :

$$\begin{aligned}\frac{d\left(N_P\tilde{n}\right)}{dt} &= \mathcal{R}_{cp}\Big(\sum_{i=2}^{\infty} i(i-1)\upsilon_{i-1} - \sum_{i=2}^{\infty} i(i-1)\upsilon_i\Big) \\ &+ \frac{\mathcal{R}_T}{2\tilde{n}}\Big(\sum_{i=0:2}^{\infty} i(i-1)(i+1)(i+2)\upsilon_{i+2} \\ &- \sum_{i=0:2}^{\infty} i^2(i-1)^2\upsilon_i\Big) \\ &+ \frac{\left(\mathcal{R}_{Zp} + \mathcal{R}_{des}\right)}{\bar{n}}\Big(\sum_{i=0:1}^{\infty} i\,(i-1)\,(i+1)\,\upsilon_{i+1} \\ &- \sum_{i=1:2}^{\infty} i^2\,(i-1)\,\upsilon_i\Big) \end{aligned} \tag{.39}$$

All terms of the equation .39 could be simplified as follows,

$$\begin{aligned}\sum_{i=2}^{\infty} i\,(i-1)\,\upsilon_{i-1} &- \sum_{i=2}^{\infty} i\,(i-1)\,\upsilon_i = \sum_{j=1}^{\infty} j\,(j+1)\,\upsilon_j \\ &- \sum_{j=1}^{\infty} j\,(j-1)\,\upsilon_j = 2\bar{n}\end{aligned}$$

$$
\begin{aligned}
\sum_{i=0}^{\infty} & \; i\,(i-1)\,(i+1)\,(i+2)\,\upsilon_{i+2} - \sum_{i=2}^{\infty} i^2\left(i-1^2\right)\upsilon_i \\
= & \sum_{j=2}^{\infty}\left(j\,(j-1)\,(j-2)\,(j-3) - j^2\,(j-1)^2\right)\upsilon_j \\
= & \sum_{j=2}^{\infty} j\,(j-1)\,((j-2)\,(j-3) - j\,(j-1))\,\upsilon_j \\
= & \sum_{j=2}^{\infty} j\,(j-1)\,(-4j+6)\,\upsilon_j \\
= & \sum_{j=2}^{\infty} j\,(j-1)\,(-4\,(j-2)-2)\,\upsilon_j \\
= & -4\sum_{j=2}^{\infty} j\,(j-1)\,(j-2)\,\upsilon_j - 2\sum_{j=2}^{\infty} j\,(j-1)\,\upsilon_j \\
= & -4\tilde{\tilde{n}} - 2\tilde{n}
\end{aligned}
\tag{.40}
$$

such as

$$
\tilde{\tilde{n}} = \sum_{i=2}^{\infty} i\,(i-1)\,(i-2)\,\upsilon_i \tag{.41}
$$

$$
\begin{aligned}
\sum_{i=1}^{\infty} & \; i\,(i-1)\,(i+1)\,\upsilon_{i+1} - \sum_{i=2}^{\infty} i^2\,(i-1)\,\upsilon_i \\
= & \sum_{j=2}^{\infty}\left(j\,(j-1)\,(j-2) - j^2\,(j-1)\right)\upsilon_j = -2\tilde{n}
\end{aligned}
$$

Finally, the Equation .39 becomes,

$$
\begin{aligned}
\frac{d(N_p\tilde{n})}{dt} &= 2\bar{n}\mathcal{R}_{cp} + \frac{\mathcal{R}_T}{2\tilde{n}}\left(-4\tilde{\tilde{n}} - 2\tilde{n}\right) + \frac{\left(\mathcal{R}_{Zp} + \mathcal{R}_{des}\right)}{\bar{n}}(-2\tilde{n}) \\
&= 2\bar{n}\mathcal{R}_{cp} - \mathcal{R}_T\left(\frac{2\tilde{\tilde{n}}}{\tilde{n}} + 1\right) + 2\frac{\tilde{n}}{\bar{n}}\left(\mathcal{R}_{Zp} + \mathcal{R}_{des}\right)
\end{aligned}
\tag{.42}
$$

Determination of $\tilde{n}$ and $\tilde{\tilde{n}}$

We suppose that the fraction of particles containing i radicals follows a Poisson distribution :

$$
\upsilon_i = (1-\alpha)\,\frac{\lambda^{i-1}}{(i-1)!}e^{-\lambda} \tag{.43}
$$

such as

$$\alpha = \upsilon_0$$

from the other hand

$$\begin{aligned}
\sum_{i=0}^{\infty} \upsilon_i &= \upsilon_0 + \sum_{i=1}^{\infty} \upsilon_i = \alpha + \sum_{i=1}^{\infty} (1-\alpha) \frac{\lambda^{i-1}}{(i-1)!} e^{-\lambda} \\
&= \alpha + (1-\alpha) e^{-\lambda} \sum_{j=0}^{\infty} \frac{\lambda^j}{j!} \\
&= 1
\end{aligned} \tag{.44}$$

hence

$$\sum_{j=0}^{\infty} \frac{\lambda^j}{j!} = e^{\lambda}$$

$\bar{n}$, $\tilde{n}$ and $\tilde{\tilde{n}}$ could be expressed as follows

$$\begin{aligned}
\bar{n} &= \sum_{i=0}^{\infty} i\upsilon_i \\
&= (1-\alpha) \sum_{i=0}^{\infty} i \frac{\lambda^{i-1}}{(i-1)!} e^{-\lambda} \\
&= (1-\alpha) \sum_{j=0}^{\infty} (j+1) \frac{\lambda^j}{j!} e^{-\lambda} \\
&= (1-\alpha) \left[\sum_{j=0}^{\infty} j \frac{\lambda^j}{j!} e^{-\lambda} + \sum_{j=0}^{\infty} \frac{\lambda^j}{j!} e^{-\lambda} \right] \\
&= (1-\alpha) \left[\sum_{j=0}^{\infty} j \frac{\lambda^j}{j!} e^{-\lambda} + 1 \right] \\
&= (1-\alpha) \left[\lambda \sum_{j=0}^{\infty} \frac{\lambda^{j-1}}{(j-1)!} e^{-\lambda} + 1 \right] \\
\bar{n} &= (1-\alpha)(\lambda + 1)
\end{aligned} \tag{.45}$$

$$
\begin{aligned}
\tilde{n} &= \sum_{i=0}^{\infty} i\,(i-1)\,\upsilon_i \\
&= (1-\alpha)\sum_{i=0}^{\infty} i\,(i-1)\,\frac{\lambda^{i-1}}{(i-1)!}e^{-\lambda} \\
&= (1-\alpha)\sum_{i=0}^{\infty} i\frac{\lambda^{i-1}}{(i-2)!}e^{-\lambda} \\
&= (1-\alpha)\sum_{j=0}^{\infty} (j+2)\,\frac{\lambda^{j+1}}{j!}e^{-\lambda} \\
&= (1-\alpha)\sum_{j=0}^{\infty} j\frac{\lambda^{j+1}}{j!}e^{-\lambda} + \underbrace{2\lambda\sum_{j=0}^{\infty}(1-\alpha)\,\frac{\lambda^{j}}{j!}e^{-\lambda}}_{2\lambda(1-\alpha)} \\
&= (1-\alpha)\sum_{j=0}^{\infty} \frac{\lambda^{j+1}}{(j-1)!}e^{-\lambda} + 2\lambda\,(1-\alpha) \\
&= (1-\alpha)\sum_{i=0}^{\infty} \frac{\lambda^{i+2}}{i!}e^{-\lambda} + 2\lambda\,(1-\alpha) \\
&= (1-\alpha)\,\lambda^2\sum_{i=0}^{\infty} \frac{\lambda^{i}}{i!}e^{-\lambda} + 2\lambda\,(1-\alpha) \\
&= \lambda^2\,(1-\alpha) + 2\lambda\,(1-\alpha) \\
\tilde{n} &= (1-\alpha)\,\lambda\,(\lambda+2) \qquad (.46)
\end{aligned}
$$

$$
\begin{aligned}
\tilde{\bar{n}} &= \sum_{i=0}^{\infty} i\,(i-1)\,(i-2)\,\upsilon_i \\
&= (1-\alpha)\sum_{i=0:3}^{\infty} i\,(i-1)\,(i-2)\,\frac{\lambda^{i-1}}{(i-1)!}e^{-\lambda} \\
&= (1-\alpha)\sum_{i=3}^{\infty} i\frac{\lambda^{i-1}}{(i-3)!}e^{-\lambda} \\
&= (1-\alpha)\sum_{j=0}^{\infty} (j+3)\,\frac{\lambda j+2}{j!}e^{-\lambda} \\
&= (1-\alpha)\sum_{j=0}^{\infty} j\frac{\lambda^{j+2}}{j!}e^{-\lambda} + \underbrace{3\lambda^2\sum_{j=0}^{\infty}(1-\alpha)\,\frac{\lambda^j}{j!}e^{-\lambda}}_{3\lambda^2(1-\alpha)} \\
&= (1-\alpha)\sum_{j=0}^{\infty}\frac{\lambda^{j+2}}{(j-1)!}e^{-\lambda}+3\lambda^2\,(1-\alpha) \\
&= (1-\alpha)\sum_{i=0}^{\infty}\frac{\lambda^{i+3}}{i!}e^{-\lambda}+3\lambda^2\,(1-\alpha) \\
&= (1-\alpha)\,\lambda^3\sum_{i=0}^{\infty}\frac{\lambda^i}{i!}e^{-\lambda}+3\lambda^2\,(1-\alpha) \\
&= \lambda^3\,(1-\alpha)+3\lambda^2\,(1-\alpha) \\
\tilde{\bar{n}} &= (1-\alpha)\,\lambda^2\,(\lambda+3) \qquad (.47)
\end{aligned}
$$

Determination of λ

By deviding $\tilde{n}$ by $\bar{n}$ we get a second order equation as follows,

$$
\frac{\tilde{n}}{\bar{n}} = \frac{(1-\alpha)\,\lambda\,(\lambda+2)}{(1-\alpha)\,(\lambda+1)} = \frac{\lambda\,(\lambda+2)}{(\lambda+1)}
$$

$$
\frac{\tilde{n}}{\bar{n}}\,(\lambda+1) = \lambda\,(\lambda+2)
$$

$$
\lambda^2 + \lambda\left(2-\frac{\tilde{n}}{\bar{n}}\right) - \frac{\tilde{n}}{\bar{n}} = 0 \qquad (.48)
$$

The positive solution is :

$$
\lambda = \frac{\tilde{n}}{2\bar{n}} - 1 + \sqrt{1+\left(\frac{\tilde{n}}{2\bar{n}}\right)^2} \qquad (.49)
$$

To get the expression of $\tilde{\bar{n}}$ let's divide $\tilde{\bar{n}}$ by $\tilde{n}$

$$\frac{\tilde{\tilde{n}}}{\tilde{n}} = \frac{(1-\alpha)\,\lambda^2\,(\lambda+3)}{(1-\alpha)\,\lambda\,(\lambda+2)} = \frac{\lambda^2+3\lambda}{(\lambda+2)}$$

By using the equation .48 we get ,

$$\tilde{\tilde{n}} = \tilde{n}\left(\frac{\frac{\tilde{\tilde{n}}}{\tilde{n}} + \lambda\left(1+\frac{\tilde{n}}{\tilde{n}}\right)}{(\lambda+2)}\right) \tag{.50}$$